Fiber Orientation Distribution Functions and Orientation Tensors for Different Material Symmetries

Maher Moakher and Peter J. Basser

Abstract In this paper we give closed-form expressions of the orientation tensors up to the order four associated with some axially-symmetric orientation distribution functions (ODF), including the well-known von Mises-Fisher, Watson, and de la Vallée Poussin ODFs. Each is characterized by a mean direction and a concentration parameter. Then, we use these elementary ODFs as building blocks to construct new ones with a specified material symmetry and derive the corresponding orientation tensors. For a general ODF we present a systematic way of calculating the corresponding orientation tensors from certain coefficients of the expansion of the ODF in spherical harmonics.

Mathematics Subject Classification (2010): 74A40, 74E10, 62H11, 92C10

1 Introduction

Fibrous composites are ubiquitous in nature and occur over a wide range of length scales. While there are familiar examples in engineering, materials sciences, and geophysics, in biology, they arise as nanoscale fibrous macromolecular systems, sub-microscopic fibrous bundles, and even macroscopic fibrous tissues and organs. There is an increasing appreciation and desire to describe, predict, and measure material and transport processes within these complex systems. Central to achieving this goal is developing a mathematical and statistical framework like the one

M. Moakher (✉)
Laboratory for Mathematical and Numerical Modeling in Engineering Science, National Engineering School at Tunis, University of Tunis El Manar, ENIT-LAMSIN, B.P. 37, 1002 Tunis-Belvédère, Tunisia
e-mail: maher.moakher@gmail.com

P.J. Basser
Section on Tissue Biophysics & Biomimetics, PPITS, NICHD, National Institutes of Health, 13 South Drive, Bldg. 13, Rm. 3W16, Bethesda, MD 20892-5772, USA
e-mail: pjbasser@helix.nih.gov

I. Hotz, T. Schultz (eds.), *Visualization and Processing of Higher Order Descriptors for Multi-Valued Data*, Mathematics and Visualization,
DOI 10.1007/978-3-319-15090-1_3

presented here, from which one can build constitutive laws and more precise, accurate, and predictive models of material behavior. In the medical imaging field, there has been much interest determining orientation distribution functions (ODF) in brain white matter. For this application, the ODFs we consider and propose here can be explicitly included in models of nerve fiber orientation within an imaging voxel, whose parameters could be measured or estimated from MRI data.

The microscopic description of fiber orientation in fibrous materials, which are made of a large collection of rod-like objects, is embodied in the ODF, which is a non-negative function ρ defined on the unit sphere S^2 of $\mathbb{R}^3$. It is normalized so that $\int_{S^2} \rho(\mathbf{n})\, d\sigma = 1$, where $d\sigma$ is the area element in S^2 and $\mathbf{n}$ is a generic vector on the unit sphere S^2 that can be parametrized by spherical coordinates as $\mathbf{n} = (\cos\theta \sin\phi,\ \sin\theta \sin\phi,\ \cos\phi)^T$ with $0 \leq \theta \leq 2\pi$ and $0 \leq \phi \leq \pi$. If ρ satisfies $\rho(\mathbf{n}) = \rho(-\mathbf{n})$, then ρ is said to be antipodally symmetric.

Since the work of Advani and Tucker [1], orientation tensors of even orders have been used to describe the orientation of fibers at the macroscopic scale. For a given positive integer k, the kth order orientation tensor is given by the expected value, with respect to the orientation distribution function ρ, over all orientations $\mathbf{n} \in S^2$:

$$\langle \mathbf{n}^{\otimes k} \rangle_\rho := \int_{S^2} \rho(\mathbf{n}) \mathbf{n}^{\otimes k}\, d\sigma, \tag{1}$$

where, $\mathbf{n}^{\otimes k}$ denotes the kth-power tensor product of $\mathbf{n}$ defined by

$$\mathbf{n}^{\otimes k} = \underbrace{\mathbf{n} \otimes \mathbf{n} \otimes \cdots \otimes \mathbf{n}}_{k \text{ times}}.$$

Orientation tensors enjoy certain properties that follow immediately from their definition (1). First, the kth order orientation tensor $\langle \mathbf{n}^{\otimes k} \rangle_\rho$ is totally symmetric, i.e., its components satisfy

$$(\langle \mathbf{n}^{\otimes k} \rangle_\rho)_{i_1,\cdots,i_k} = (\langle \mathbf{n}^{\otimes k} \rangle_\rho)_{i_{\sigma(1)},\cdots,i_{\sigma(k)}},$$

for all permutations $\sigma(\cdot)$ of the integers $1, \cdots, k$. Second, since $\mathbf{n}$ is a unit vector, all the components of $\langle \mathbf{n}^{\otimes k} \rangle_\rho$ are less than or equal to one in absolute value. Third, the contraction of the kth order orientation tensor with respect to any two indices is the $(k-2)$th order orientation tensor, i.e.,

$$(\langle \mathbf{n}^{\otimes k} \rangle_\rho)_{i_1,\cdots,i_{k-2},j,j} = (\langle \mathbf{n}^{\otimes k-2} \rangle_\rho)_{i_1,\cdots,i_{k-2}}.$$

Furthermore, the trace of even-order orientation tensors $\langle \mathbf{n}^{\otimes 2k} \rangle_\rho$ is equal to one

$$(\langle \mathbf{n}^{\otimes 2k} \rangle_\rho)_{i_1,\cdots,i_k,i_1,\cdots,i_k} = 1,$$

and the complete contraction of odd-order orientation tensors $\langle \mathbf{n}^{\otimes 2k+1} \rangle_\rho$ is equal to the orientation tensor of the first order, i.e.,

$$(\langle \mathbf{n}^{\otimes 2k+1} \rangle_\rho)_{i_1,\cdots,i_k,i_1,\cdots,i_k,j} = (\langle \mathbf{n} \rangle_\rho)_j .$$

Any ODF ρ can be (uniquely) decomposed into an antipodally symmetric part ρ^s and an antipodally skew-symmetric part ρ^a according to

$$\rho(\mathbf{n}) = \rho^s(\mathbf{n}) + \rho^a(\mathbf{n}), \tag{2}$$

where

$$\rho^s(\mathbf{n}) := \tfrac{1}{2}(\rho(\mathbf{n}) + \rho(-\mathbf{n})) \text{ and } \rho^a(\mathbf{n}) := \tfrac{1}{2}(\rho(\mathbf{n}) - \rho(-\mathbf{n})).$$

It should be noted that the antipodally symmetric part ρ^s is always an ODF, i.e., it is a non-negative function in S^2 and its integral over S^2 is equal to one. In general, the antipodally skew-symmetric part is not, however, an orientation distribution function.

By exploiting the fact that integration over S^2 is invariant under the change of variable $\mathbf{n} \to -\mathbf{n}$ it follows that for k even we have

$$\int_{S^2} \rho(\mathbf{n})\mathbf{n}^{\otimes k}\, d\sigma = \int_{S^2} \rho(-\mathbf{n})\mathbf{n}^{\otimes k}\, d\sigma = \int_{S^2} \tfrac{1}{2}(\rho(\mathbf{n}) + \rho(-\mathbf{n}))\mathbf{n}^{\otimes k}\, d\sigma,$$

and that for k odd we have

$$\int_{S^2} \rho(\mathbf{n})\mathbf{n}^{\otimes k}\, d\sigma = -\int_{S^2} \rho(-\mathbf{n})\mathbf{n}^{\otimes k}\, d\sigma = \int_{S^2} \tfrac{1}{2}(\rho(\mathbf{n}) - \rho(-\mathbf{n}))\mathbf{n}^{\otimes k}\, d\sigma.$$

Therefore, even-order orientation tensors depend only on the antipodally symmetric part of ρ and odd-order orientation tensors depend only on the antipodally skew symmetric part of ρ. As a consequence, when ρ is antipodally symmetric all odd-order orientation tensors vanish. The orientation tensor of order k, $\langle \mathbf{n}^{\otimes k} \rangle_\rho$, is also called a *fabric tensor of the first kind of rank k* [16].

For an ODF $\rho(\mathbf{n})$ defined on the unit sphere S^2, one can consider the kth order approximation

$$\tilde{\rho}(\mathbf{n}) := \mathbb{C}_0 + \mathbb{C}_1 \cdot \mathbf{n} + \mathrm{tr}(\mathbb{C}_2 \langle \mathbf{n}^{\otimes 2} \rangle_\rho) + \mathrm{tr}(\mathbb{C}_3 \langle \mathbf{n}^{\otimes 3} \rangle_\rho) + \cdots + \mathrm{tr}(\mathbb{C}_k \langle \mathbf{n}^{\otimes k} \rangle_\rho),$$

where the coefficients $\mathbb{C}_i$, $i = 0, \ldots, k$, each of which is a totally symmetric tensor of order i, are determined so that the least-squares functional

$$\mathscr{E}(\rho) := \int_{S^2} [\rho(\mathbf{n}) - \tilde{\rho}(\mathbf{n})]^2 \, d\sigma,$$

is minimized. However, as explained in the seminal paper of Kanatani [16], these coefficients tensors are not uniquely defined. The reason is that the even-order tensors $1, \mathbf{n}^{\otimes 2}, \mathbf{n}^{\otimes 4} \ \ldots$ are not linearly independent, and similarly, the odd-order tensors $\mathbf{n}, \mathbf{n}^{\otimes 3} \ \ldots$ are not linearly independent. In fact, since $\|\mathbf{n}\| = 1$, $\mathbf{n}^{\otimes l}$ can be obtained from $\mathbf{n}^{\otimes k}$, with $k \geq l + 2$, by repeated contractions.

We note that if $\rho(\mathbf{n})$ is antipodally symmetric, which is the condition that we will consider next, then all odd-order coefficient tensors vanish. Let V_l be the vector space of functions defined on S^2 spanned by $\mathbf{n}^{\otimes l}$. Then, because of what we stated earlier on the linear dependence of $1, \mathbf{n}^{\otimes 2}, \mathbf{n}^{\otimes 4} \ \ldots$, we have $V_0 \subset V_2 \subset V_4 \ldots$. Therefore, if one wants to approximate $\rho(\mathbf{n})$ up to order k (even), then it suffices to simply consider an approximation of the form

$$\rho(\mathbf{n}) \sim \frac{1}{4\pi} F_{i_1 \cdots i_k} n_{i_1} \cdots n_{i_k}, \tag{3}$$

where $F_{i_1 \cdots i_k}$ are the components of a kth order totally symmetric tensor called the *fabric tensor of the second kind of rank k* [16]. The fabric tensors of the second kind of rank 0, 2, and 4 are, respectively

$$\mathscr{F} = 1, \ \mathbf{F} = \frac{15}{2}\left[\langle \mathbf{n}^{\otimes 2} \rangle_\rho - \tfrac{1}{5}\mathbf{I}\right], \ \mathbb{F} = \frac{315}{8}\left[\langle \mathbf{n}^{\otimes 4} \rangle_\rho - \tfrac{1}{3}(\mathbf{I} \otimes \langle \mathbf{n}^{\otimes 2} \rangle_\rho)^s + \tfrac{1}{7}(\mathbf{I} \otimes \mathbf{I})^s\right].$$

Here and throughout the paper, $\mathbf{I}$ denotes the (second-order) identity tensor, and the superscript ^{s} on a tensor indicates taking the totally symmetric part of that tensor.

Because the approximation (3) has a compact form, the number of tensor components needed for the computation is minimal. However, to get a higher-order approximation one must recompute the tensor. By a Gram-Schmidt process, we can get the orthogonal decomposition of $V_k = V_k' \oplus V_{k-2}' \oplus \cdots \oplus V_0'$ where $V_0' = V_0$ and V_l' is the orthogonal complement of V_{l-2} in V_l with respect to the $L^2(S^2)$-inner product. Then, using this orthogonal decomposition, we obtain the more practical approximation of $\rho(\mathbf{n})$ [15, 16]:

$$\rho(\mathbf{n}) \sim \frac{1}{4\pi}\left[\mathscr{D} + \operatorname{tr}(\mathbf{D}\langle \mathbf{n}^{\otimes 2} \rangle_\rho) + \operatorname{tr}(\mathbb{D}\langle \mathbf{n}^{\otimes 4} \rangle_\rho) + \cdots\right]. \tag{4}$$

The coefficients $\mathscr{D}$, $\mathbf{D}$, and $\mathbb{D}$ are called the *fabric tensors of the third kind* of rank 0, 2, and 4, respectively. They are given by

$$\mathscr{D} = 1, \ \mathbf{D} = \frac{15}{2}\left[\langle \mathbf{n}^{\otimes 2} \rangle_\rho - \tfrac{1}{3}\mathbf{I}\right], \ \mathbb{D} = \frac{315}{8}\left[\langle \mathbf{n}^{\otimes 4} \rangle_\rho - \tfrac{3}{7}(\mathbf{I} \otimes \langle \mathbf{n}^{\otimes 2} \rangle_\rho)^s + \tfrac{1}{35}(\mathbf{I} \otimes \mathbf{I})^s\right].$$

In the field of diffusion MRI, high angular diffusion resolution imaging (HARDI) is a commonly used modality for non-invasively probing water diffusion in fibrous biological tissues such as muscle and brain white matter. HARDI encompasses

several techniques such as Q-ball imaging [31], diffusion orientation transform MRI [24], and spherical deconvolution MRI [30]. In general, these techniques produce a function defined on the unit sphere. Various high-order tensor decompositions have been used for approximating such functions. The reader is referred to the recent review article [28] on the use of higher-order tensors in diffusion imaging. We here particularly mention the work of Özarslan and Mareci [23] who employed an approximation of the form (3), and the work of Florack and co-authors [9, 10] who used an approximation of the form (4).

We mention that orientation tensors of even order have been widely used in the macroscopic description of short-fiber composites [2, 14], fiber suspensions [7], damage mechanics [25, 33], etc. For classical solids and fluids, the even-order orientation tensors suffice for the macroscopic description of such media. However, there are natural and man-made materials that exhibit chiral behavior, i.e., they are not invariant under inversion. Such materials are called chiral, noncentrosymmetric, or hemitropic [17]. For instance, quartz, biological molecules such as the DNA double helix, and composites with helical or screw-shaped inclusions, polar chiral materials [6, 12, 22], and chiral metamaterials [34] all show different behaviors for opposite directions. Material properties such as piezoelectricity and pyroelectricity are represented by odd-order tensors [17]. It is therefore necessary to use odd-order orientation tensors as well for the macroscopic description of such properties for these types of media. We should also mention that odd-order orientation tensors are necessary for dealing with singularities in fiber arrangements and in fiber splaying and merging. Furthermore, in the work of Liu et al. [18], odd-order diffusion tensors are considered for the measurement of the phases of magnetic resonance signals.

In the remainder of the paper, we will give the expressions of the orientation tensors up to the fourth order for ODFs with some prescribed material symmetry classes. The notation that will be used is described below.

Let $\mathscr{E}^3$ denote the three-dimensional Euclidean space and let $\{\mathbf{e}_i\}_{i=1,2,3}$ be an orthonormal basis of it. Any vector $\mathbf{v}$ in $\mathscr{E}^3$ can be represented as $\mathbf{v} = v_i \mathbf{e}_i$. The inner product of two vectors $\mathbf{a}$ and $\mathbf{b}$ is denoted by $\mathbf{a} \cdot \mathbf{b}$.

A second-order tensor $\mathbf{T}$ of the three-dimensional space $\mathscr{E}^3$ is a linear map that assigns to each vector in $\mathscr{E}^3$ a vector in $\mathscr{E}^3$. We denote by $\mathbf{u} \otimes \mathbf{v}$ the second-order tensor that assigns to a vector $\mathbf{w}$ the vector $(\mathbf{v} \cdot \mathbf{w})\mathbf{u}$. A second-order tensor can thus be represented as $\mathbf{T} = T_{ij} \mathbf{e}_i \otimes \mathbf{e}_j$. A second-order tensor $\mathbf{T}$ is symmetric if $T_{ij} = T_{ji}$ for all $i, j = 1, 2, 3$. The tensor product $\mathbf{a} \otimes \mathbf{b}$ of two vectors is the tensor that assigns to each vector $\mathbf{u}$ the vector $(\mathbf{b} \cdot \mathbf{u})\mathbf{a}$. In components $(\mathbf{a} \otimes \mathbf{b})_{ij} = a_i b_j$.

A third-order tensor T can be seen as a linear map that assigns a vector to each second-order tensor. A third-order tensor admits the representation $\mathsf{T} = T_{ijk} \mathbf{e}_i \otimes \mathbf{e}_j \otimes \mathbf{e}_k$. This tensor is said to be symmetric in the last two indices if $T_{ijk} = T_{ikj}$ for all $i, j, k = 1, 2, 3$, and totally symmetric if in addition $T_{ijk} = T_{jik}$ for all $i, j, k = 1, 2, 3$.

A fourth-order tensor $\mathbb{T}$ can be seen as a linear map that assigns to each second-order tensor a second-order tensor. A fourth-order tensor admits the representation $\mathbb{T} = T_{ijkl} \mathbf{e}_i \otimes \mathbf{e}_j \otimes \mathbf{e}_k \otimes \mathbf{e}_l$. This tensor is said to possess the minor symmetries

if $T_{ijkl} = T_{jikl} = T_{ijlk}$ for all $i, j, k, l = 1, 2, 3$, the major symmetry if $T_{ijkl} = T_{klij}$ for all $i, j, k, l = 1, 2, 3$, and total symmetry if in addition to the minor and major symmetries it satisfies $T_{ijkl} = T_{ikjl}$ for all $i, j, k, l = 1, 2, 3$. Any fourth-order tensor $\mathbb{T}$ possessing the minor and major symmetries can be decomposed, in a unique manner, into its totally symmetric part $\mathbb{T}^s$ and its asymmetric part $\mathbb{T}^a$ as: $\mathbb{T} = \mathbb{T}^s + \mathbb{T}^a$. The components of the totally symmetric and asymmetric parts are [3, 21]

$$T^s_{ijkl} = \tfrac{1}{3}(T_{ijkl} + T_{ikjl} + T_{ilkj}), \qquad T^a_{ijkl} = \tfrac{1}{3}(2T_{ijkl} - T_{ikjl} - T_{ilkj}). \tag{5}$$

Let $\mathbb{I}$ denote the fourth-order identity tensor whose components are given by $I_{ijkl} = \frac{1}{2}(\delta_{ik}\delta_{jl} + \delta_{il}\delta_{jk})$. Then the components of its totally symmetric part $\mathbb{I}^s$ are $I^s_{ijkl} = \frac{1}{3}(\delta_{ik}\delta_{jl} + \delta_{il}\delta_{jk} + \delta_{ij}\delta_{kl})$, and the components of its asymmetric part $\mathbb{I}^a$ are $I^a_{ijkl} = \frac{1}{6}(\delta_{ik}\delta_{jl} + \delta_{il}\delta_{jk} - 2\delta_{ij}\delta_{kl})$.

We note that vectors and second-order tensors are easily dealt with by using linear algebra operations. This is not the case for third- and fourth-order tensors. We therefore introduce a (non-physical) six-dimensional space $\hat{\mathscr{E}}$ so that the usual linear algebra operations can be used for the manipulation of third-order tensors that are symmetric with respect to the last two indices and fourth-order tensors possessing the minor symmetries.

Let $\hat{\mathbf{e}}_1 = \mathbf{e}_1 \otimes \mathbf{e}_1$, $\hat{\mathbf{e}}_2 = \mathbf{e}_2 \otimes \mathbf{e}_2$, $\hat{\mathbf{e}}_3 = \mathbf{e}_3 \otimes \mathbf{e}_3$, $\hat{\mathbf{e}}_4 = 2^{-1/2}(\mathbf{e}_2 \otimes \mathbf{e}_3 + \mathbf{e}_3 \otimes \mathbf{e}_2)$, $\hat{\mathbf{e}}_5 = 2^{-1/2}(\mathbf{e}_1 \otimes \mathbf{e}_3 + \mathbf{e}_3 \otimes \mathbf{e}_1)$ and $\hat{\mathbf{e}}_6 = 2^{-1/2}(\mathbf{e}_1 \otimes \mathbf{e}_2 + \mathbf{e}_2 \otimes \mathbf{e}_1)$. Then any third-order tensor $\mathsf{T} = T_{ijk}\mathbf{e}_i \otimes \mathbf{e}_j \otimes \mathbf{e}_k$ with $T_{ijk} = T_{ikj}$ can be represented by

$$\hat{\mathsf{T}} = \hat{T}_{i\alpha}\mathbf{e}_i \otimes \hat{\mathbf{e}}_\alpha,$$

where the Latin indices range from 1 to 3 and the Greek indices run from 1 to 6. Similarly, any fourth-order tensor $\mathbb{T} = T_{ijkl}\mathbf{e}_i \otimes \mathbf{e}_j \otimes \mathbf{e}_k \otimes \mathbf{e}_l$ with $T_{ijkl} = T_{jikl} = T_{ijlk}$ can be represented by

$$\hat{\mathbb{T}} = \hat{T}_{\alpha\beta}\hat{\mathbf{e}}_\alpha \otimes \hat{\mathbf{e}}_\beta.$$

In this way, the fourth-order identity tensor $\mathbb{I}$ is represented by, $\hat{\mathbf{I}}$, the second-order identity tensor in $\hat{\mathscr{E}}$ whose components are $\hat{I}_{\alpha\beta} = \delta_{\alpha\beta}$.

2 Isotropic, Transversely Isotropic, and Uniform ODFs

The isotropic ODF is given by

$$\rho^{\mathrm{iso}}(\mathbf{n}) = \frac{1}{4\pi}. \tag{6}$$

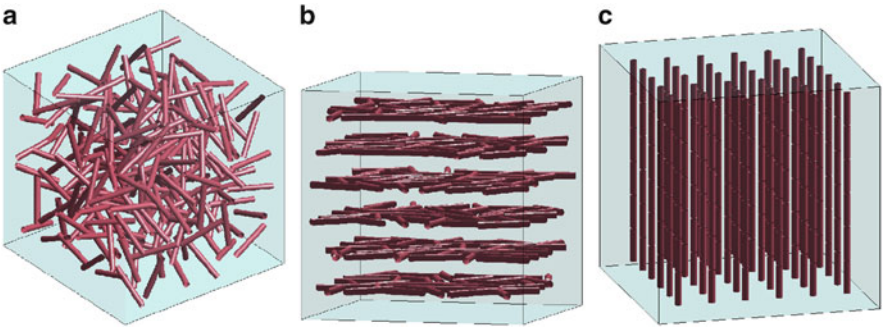

Fig. 1 (**a**) Spatial randomly oriented fibers, (**b**) planar randomly oriented fibers, (**c**) totally aligned fibers

The isotropic orientation averages of $\mathbf{n}^{\otimes 2}$ and $\mathbf{n}^{\otimes 4}$ are given by

$$\langle \mathbf{n}^{\otimes 2} \rangle^{\text{iso}} := \int_{S^2} \rho^{\text{iso}}(\mathbf{n}) \mathbf{n}^{\otimes 2} \, d\sigma = \tfrac{1}{3}\mathbf{I}, \tag{7}$$

and

$$\langle \mathbf{n}^{\otimes 4} \rangle^{\text{iso}} := \int_{S^2} \rho^{\text{iso}}(\mathbf{n}) \mathbf{n}^{\otimes 4} \, d\sigma = \tfrac{1}{5}\mathbb{I}^s, \tag{8}$$

where $\mathbb{I}^s$ is the totally symmetric part (defined by $(5)_1$) of the fourth-order identity tensor $\mathbb{I}$. The isotropic distribution (6) represents a uniform distribution of orientations on the unit sphere S^2. This distribution corresponds to fibers that are randomly oriented as depicted in Fig. 1a.

There are two other special distributions that need to be mentioned here. First, the distribution

$$\rho^{\text{iso},\mathbf{m}}(\mathbf{n}) = \frac{1}{2\pi}\delta(\mathbf{n} \cdot \mathbf{m}), \tag{9}$$

represents a uniform distribution of orientations in the plane perpendicular to $\mathbf{m}$, where $\mathbf{m}$ is a unit vector and $\delta(\cdot)$ denotes the Dirac delta function. This distribution corresponds to randomly oriented fibers in planes perpendicular to $\mathbf{m}$, see Fig. 1b. The second- and fourth-order orientation tensors associated with (9) are

$$\langle \mathbf{n}^{\otimes 2} \rangle^{\text{iso},\mathbf{m}} := \int_{S^2} \rho^{\text{iso},\mathbf{m}}(\mathbf{n}) \mathbf{n}^{\otimes 2} \, d\sigma = \tfrac{1}{2}(\mathbf{p}^{\otimes 2} + \mathbf{q}^{\otimes 2}),$$

and

$$\langle \mathbf{n}^{\otimes 4} \rangle^{\mathrm{iso},\mathbf{m}} := \int_{S^2} \rho^{\mathrm{iso},\mathbf{m}}(\mathbf{n}) \mathbf{n}^{\otimes 4} \, d\sigma = \tfrac{1}{8} \big[3\mathbf{p}^{\otimes 4} + 3\mathbf{q}^{\otimes 4} + \mathbf{p}^{\otimes 2} \otimes \mathbf{q}^{\otimes 2} + \mathbf{q}^{\otimes 2} \otimes \mathbf{p}^{\otimes 2} + (\mathbf{p} \otimes \mathbf{q})^{\otimes 2} + (\mathbf{q} \otimes \mathbf{p})^{\otimes 2} + \mathbf{p} \otimes \mathbf{q}^{\otimes 2} \otimes \mathbf{p} + \mathbf{q} \otimes \mathbf{p}^{\otimes 2} \otimes \mathbf{q} \big],$$

where $\mathbf{p}$ and $\mathbf{q}$ are any two orthogonal unit vectors in the plane perpendicular to $\mathbf{m}$.

Second, the distribution

$$\rho^{\mathbf{m}}(\mathbf{n}) = \frac{\delta(1 - (\mathbf{n} \cdot \mathbf{m})^2)}{4\pi \sqrt{1 - (\mathbf{n} \cdot \mathbf{m})^2}}, \tag{10}$$

represents orientations totally aligned with $\mathbf{m}$. This distribution corresponds to fibers oriented along $\mathbf{m}$, see Fig. 1c. We note that this orientation distribution can simply be expressed as $\rho^{\mathbf{m}}(\mathbf{n}) = \boldsymbol{\delta}_{\mathbf{m}}(\mathbf{n})$, where $\boldsymbol{\delta}_{\mathbf{m}}(\cdot)$ is the spherical delta function defined such that for any functions f on S^2 we have

$$\int_{S^2} \boldsymbol{\delta}_{\mathbf{m}}(\mathbf{n}) f(\mathbf{n}) \, d\sigma = f(\mathbf{m}).$$

It is given by $\boldsymbol{\delta}_{\mathbf{m}}(\mathbf{n}) = \frac{1}{\sin\phi} \delta(\theta - \theta_0) \delta(\phi - \phi_0)$ where (θ, ϕ) and (θ_0, ϕ_0) are the spherical coordinates of $\mathbf{n}$ and $\mathbf{m}$, respectively, see e.g., [29, p. 211]. The second- and fourth-order orientation tensors associated with (10) are

$$\langle \mathbf{n}^{\otimes 2} \rangle^{\mathbf{m}} := \int_{S^2} \rho^{\mathbf{m}}(\mathbf{n}) \mathbf{n}^{\otimes 2} \, d\sigma = \mathbf{m}^{\otimes 2}, \tag{11}$$

and

$$\langle \mathbf{n}^{\otimes 4} \rangle^{\mathbf{m}} := \int_{S^2} \rho^{\mathbf{m}}(\mathbf{n}) \mathbf{n}^{\otimes 4} \, d\sigma = \mathbf{m}^{\otimes 4}. \tag{12}$$

3 Axially-Symmetric ODFs

We say that an ODF $\varrho_{\mathbf{m}}(\cdot)$ is axially symmetric with respect to $\mathbf{m} \in S^2$ if $\varrho_{\mathbf{m}}(\mathbf{Rn}) = \varrho_{\mathbf{m}}(\mathbf{n})$ for all (proper) rotations $\mathbf{R}$ about the vector $\mathbf{m}$. The ODF $\varrho_{\mathbf{m}}(\cdot)$ is also called *transversely hemitropic* with $\mathbf{m}$ as the direction of transverse hemitropy. In this case, there exists a positive function $\tilde{\varrho}(\cdot)$ defined on the interval $[0, \pi]$ such that

$$\varrho_{\mathbf{m}}(\mathbf{n}) = \tilde{\varrho}(\Phi), \tag{13}$$

where $\cos\Phi = \mathbf{m}\cdot\mathbf{n}$. As $\varrho_{\mathbf{m}}(\cdot)$ is normalized, the function $\tilde{\varrho}(\cdot)$ further satisfies

$$2\pi\int_0^\pi \tilde{\varrho}(\Phi)\sin\Phi\, d\Phi = 1.$$

If, in addition the ODF $\varrho_{\mathbf{m}}(\cdot)$ is antipodally symmetric, which is the case when $\tilde{\varrho}(\Phi) = \tilde{\varrho}(\pi - \Phi)$ for all $\Phi \in [0,\pi]$, then the ODF $\varrho_{\mathbf{m}}(\cdot)$ is called transversely isotropic with $\mathbf{m}$ as the direction of transverse isotropy.

The first-order orientation tensor, corresponding to the axially symmetric distribution $\varrho_{\mathbf{e}_3}$, is

$$\langle\mathbf{n}\rangle_{\varrho_{\mathbf{e}_3}} := \int_{S^2}\varrho_{\mathbf{e}_3}(\mathbf{n})\mathbf{n}\, d\sigma = \begin{bmatrix}0\\0\\A\end{bmatrix},$$

and the corresponding second-order orientation tensor is

$$\langle\mathbf{n}^{\otimes 2}\rangle_{\varrho_{\mathbf{e}_3}} := \int_{S^2}\varrho_{\mathbf{e}_3}(\mathbf{n})\mathbf{n}^{\otimes 2}\, d\sigma = \begin{bmatrix}B & 0 & 0\\ 0 & B & 0\\ 0 & 0 & 1-2B\end{bmatrix},$$

where

$$A = 2\pi\int_0^\pi \cos\Phi\sin\Phi\,\tilde{\varrho}(\Phi)\, d\Phi, \qquad B = \pi\int_0^\pi \sin^3\Phi\,\tilde{\varrho}(\Phi)\, d\Phi. \tag{14}$$

The corresponding third-order orientation tensor,

$$\langle\mathbf{n}^{\otimes 3}\rangle_{\varrho_{\mathbf{e}_3}} := \int_{S^2}\varrho_{\mathbf{e}_3}(\mathbf{n})\mathbf{n}^{\otimes 3}\, d\sigma,$$

has the matrix representation

$$\begin{bmatrix}0 & 0 & 0 & 0 & \sqrt{2}C & 0\\ 0 & 0 & 0 & \sqrt{2}C & 0 & 0\\ C & C & A-2C & 0 & 0 & 0\end{bmatrix},$$

where

$$C = \pi\int_0^\pi \cos\Phi\sin^3\Phi\,\tilde{\varrho}(\Phi)\, d\Phi. \tag{15}$$

Similarly, the corresponding fourth-order orientation tensor,

$$\langle \mathbf{n}^{\otimes 4} \rangle_{\varrho_{\mathbf{e}_3}} := \int_{S^2} \rho_{\varrho \mathbf{e}_3}(\mathbf{n}) \mathbf{n}^{\otimes 4} \, d\sigma,$$

has the 6D second-order tensor representation

$$\begin{bmatrix} 3D & D & F & 0 & 0 & 0 \\ D & 3D & F & 0 & 0 & 0 \\ F & F & E & 0 & 0 & 0 \\ 0 & 0 & 0 & 2F & 0 & 0 \\ 0 & 0 & 0 & 0 & 2F & 0 \\ 0 & 0 & 0 & 0 & 0 & 2D \end{bmatrix},$$

where

$$D = \tfrac{1}{4}\pi \int_0^\pi \sin^5 \Phi \, \tilde{\varrho}(\Phi) \, d\Phi, \tag{16a}$$

$$E = 2\pi \int_0^\pi \cos^4 \Phi \sin^5 \Phi \, \tilde{\varrho}(\Phi) \, d\Phi, \tag{16b}$$

$$F = \pi \int_0^\pi \cos^2 \Phi \sin^3 \Phi \, \tilde{\varrho}(\Phi) \, d\Phi. \tag{16c}$$

As the trace of the fourth-order orientation tensor is equal to one, one can easily verify that $8D + E + 4F = 2\pi \int_0^\pi \sin \Phi \, \tilde{\varrho}(\Phi) \, d\Phi = 1$.

In the following subsections we will give explicit expressions of the orientation tensors up to the order four for several uni-modal axially symmetric ODFs. All these orientation distributions are characterized with the modal vector (mean axis) $\mathbf{m}$ and a concentration parameter $\kappa \in [0, \kappa_\infty)$. When the concentration parameter κ is equal to zero, the orientation distribution reduces to the isotropic distribution (6). On the other hand, when the concentration parameter κ approaches κ_∞ the orientation distribution tends to the totally aligned orientation distribution (10).

3.1 The von Mises-Fisher ODF

The widely used uni-modal orientation distribution is the Fisher distribution (also known as the von Mises-Fisher distribution), with modal vector $\mathbf{m} \in S^2$ and concentration parameter $\kappa > 0$; it is given by (see e.g., [19, 35])

$$\rho^{\mathrm{MF}}_{\mathbf{m},\kappa}(\mathbf{n}) = \frac{\xi^{\mathrm{MF}}(\kappa)}{4\pi} \exp(\kappa \mathbf{m} \cdot \mathbf{n}), \tag{17}$$

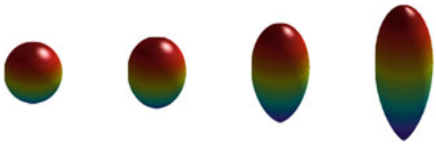

Fig. 2 Plots of the transversely hemitropic ODF (17) for $\kappa = 1, 2, 5,$ and 10

where

$$\xi^{\mathrm{MF}}(\kappa) = \frac{\kappa}{\sinh \kappa}.$$

In Fig. 2 we give plots of (17) for various values of the concentration parameter κ. It should be noted that this distribution is not invariant under the inversion of directions: $\mathbf{n} \mapsto -\mathbf{n}$, and hence it is not antipodally symmetric.

When $\mathbf{m} = \mathbf{e}_3$, the corresponding first-order orientation tensor is

$$\langle \mathbf{n} \rangle^{\mathrm{MF}}_{\mathbf{m}_3,\kappa} := \int_{S^2} \rho^{\mathrm{MF}}_{\mathbf{m}_3,\kappa}(\mathbf{n})\mathbf{n}\, d\sigma = \frac{1}{\kappa} \begin{bmatrix} 0 \\ 0 \\ \alpha(\kappa) \end{bmatrix},$$

and the corresponding second-order orientation tensor is

$$\langle \mathbf{n}^{\otimes 2} \rangle^{\mathrm{MF}}_{\mathbf{m}_3,\kappa} := \int_{S^2} \rho^{\mathrm{MF}}_{\mathbf{m}_3,\kappa}(\mathbf{n})\mathbf{n}^{\otimes 2}\, d\sigma = \frac{1}{\kappa^2} \begin{bmatrix} \alpha(\kappa) & 0 & 0 \\ 0 & \alpha(\kappa) & 0 \\ 0 & 0 & \kappa^2 - 2\alpha(\kappa) \end{bmatrix},$$

where

$$\alpha(\kappa) = \xi^{\mathrm{MF}}(\kappa) \cosh \kappa - 1.$$

The corresponding third-order orientation tensor

$$\langle \mathbf{n}^{\otimes 3} \rangle^{\mathrm{MF}}_{\mathbf{m}_3,\kappa} := \int_{S^2} \rho^{\mathrm{MF}}_{\mathbf{m}_3,\kappa}(\mathbf{n})\mathbf{n}^{\otimes 3}\, d\sigma,$$

has the matrix representation

$$\frac{1}{\kappa^3} \begin{bmatrix} 0 & 0 & 0 & 0 & \sqrt{2}\beta(\kappa) & 0 \\ 0 & 0 & 0 & \sqrt{2}\beta(\kappa) & 0 & 0 \\ \beta(\kappa) & \beta(\kappa) & \gamma(\kappa) & 0 & 0 & 0 \end{bmatrix},$$

where

$$\beta(\kappa) = (\kappa^2 + 3) - 3\xi^{\mathrm{MF}}(\kappa) \cosh \kappa,$$
$$\gamma(\kappa) = (\kappa^2 + 6)\xi^{\mathrm{MF}}(\kappa) \cosh \kappa - 3(\kappa^2 + 2).$$

Note that as the contraction of $\langle \mathbf{n}^{\otimes 3} \rangle^{\mathrm{MF}}_{\mathbf{m}_3,\kappa}$ is equal to $\langle \mathbf{n} \rangle^{\mathrm{MF}}_{\mathbf{m}_3,\kappa}$ we can verify that

$$2\beta(\kappa) + \gamma(\kappa) = \kappa^2 \alpha(\kappa).$$

Similarly, the corresponding fourth-order orientation tensor,

$$\langle \mathbf{n}^{\otimes 4} \rangle^{\mathrm{MF}}_{\mathbf{m}_3,\kappa} := \int_{S^2} \rho^{\mathrm{MF}}_{\mathbf{m}_3,\kappa}(\mathbf{n}) \mathbf{n}^{\otimes 4} \, d\sigma,$$

has the 6D second-order tensor representation

$$\frac{1}{\kappa^4} \begin{bmatrix} 3a(\kappa) & a(\kappa) & c(\kappa) & 0 & 0 & 0 \\ a(\kappa) & 3a(\kappa) & c(\kappa) & 0 & 0 & 0 \\ c(\kappa) & c(\kappa) & b(\kappa) & 0 & 0 & 0 \\ 0 & 0 & 0 & 2c(\kappa) & 0 & 0 \\ 0 & 0 & 0 & 0 & 2c(\kappa) & 0 \\ 0 & 0 & 0 & 0 & 0 & 2a(\kappa) \end{bmatrix},$$

where

$$\begin{aligned} a(\kappa) &= \kappa^2 + 3(1 - \xi^{\mathrm{MF}}(\kappa) \cosh \kappa), \\ b(\kappa) &= \kappa^4 + 12\kappa^2 + 24 - 4(\kappa^2 + 6)\xi^{\mathrm{MF}}(\kappa) \cosh \kappa, \\ c(\kappa) &= (\kappa^2 + 12)\xi^{\mathrm{MF}}(\kappa) \cosh \kappa - 5\kappa^2 - 12. \end{aligned}$$

Because the trace of even-order orientation tensors is equal to one, the three functions $a(\cdot)$, $b(\cdot)$, and $c(\cdot)$ are dependent, satisfying the relation

$$8a(\kappa) + b(\kappa) + 4c(\kappa) = \kappa^4.$$

As mentioned before, the von Mises-Fisher ODF (17) is not antipodally symmetric. Its antipodally symmetric part is given by

$$(\rho^{\mathrm{MF}}_{\mathbf{m},\kappa})^s(\mathbf{n}) = \frac{\xi^{\mathrm{MF}}(\kappa)}{4\pi} \cosh(\kappa \mathbf{m} \cdot \mathbf{n}), \tag{18}$$

and its antipodally skew-symmetric part is given by

$$(\rho^{\mathrm{MF}}_{\mathbf{m},\kappa})^a(\mathbf{n}) = \frac{\xi^{\mathrm{MF}}(\kappa)}{4\pi} \sinh(\kappa \mathbf{m} \cdot \mathbf{n}). \tag{19}$$

Plots of (18) for various values of the concentration parameter κ are shown in Fig. 3.

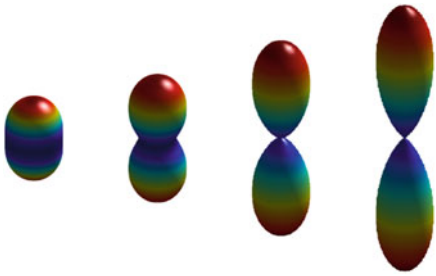

Fig. 3 Plots of the transversely isotropic ODF (18) for $\kappa = 1, 2, 5,$ and 10

All orientation tensors of even orders relative to the orientation distribution function (18) are equal to the orientation tensors of even orders relative to the orientation distribution function (17), whereas all orientation tensors of odd orders relative to the ODF (18) vanish.

3.2 The Watson ODF

The Watson distribution (also known as the Dimroth-Watson distribution) with modal vector $\mathbf{m} \in S^2$ and concentration parameter $\kappa > 0$ is given by [8]

$$\rho^{\mathrm{DW}}_{\mathbf{m},\kappa}(\mathbf{n}) = \frac{\xi^{\mathrm{DW}}(\kappa)}{4\pi} \exp(\kappa^2(\mathbf{m}\cdot\mathbf{n})^2), \tag{20}$$

where

$$\xi^{\mathrm{DW}}(\kappa) = \frac{2\kappa}{\sqrt{\pi}\,\mathrm{erfi}(\kappa)},$$

and $\mathrm{erfi}(\cdot)$ represents the imaginary error function defined by

$$\mathrm{erfi}(s) = -i\,\mathrm{erf}(is) = \frac{2s}{\sqrt{\pi}} \int_0^1 \exp(s^2t^2)\,dt.$$

This distribution can be seen as a special case of the well-known Bingham (multimodal) distribution for axial data

$$\rho_{\mathbf{K}}(\mathbf{n}) = \frac{1}{b(\mathbf{K})} \exp(\mathbf{n}\cdot\mathbf{K}\mathbf{n}),$$

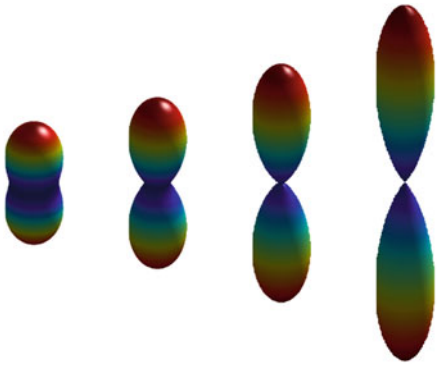

Fig. 4 Plots of the transversely isotropic ODF (20) for $\kappa = 1, \sqrt{2}, 2,$ and 3

where $\mathbf{K}$ is a symmetric matrix and $b(\mathbf{K})$ is a normalization constant. The distribution $\rho^{\mathrm{DW}}_{\mathbf{m},\kappa}(\mathbf{n})$ is transversely isotropic. Like the von Mises-Fisher distribution, the Dimroth-Watson distribution is parametrized by the concentration parameter κ. Plots of (20) for various values of the concentration parameter κ are given in Fig. 4.

When $\mathbf{m} = \mathbf{e}_3$, the corresponding second-order orientation tensor $\langle \mathbf{n}^{\otimes 2} \rangle^{\mathrm{DW}}_{\mathbf{m}_3,\kappa} := \int_{S^2} \rho^{\mathrm{DW}}_{\mathbf{m}_3,\kappa}(\mathbf{n}) \mathbf{n}^{\otimes 2} \, d\sigma$ is given by

$$\frac{1}{4\kappa^2} \begin{bmatrix} \tilde{\alpha}(\kappa) & 0 & 0 \\ 0 & \tilde{\alpha}(\kappa) & 0 \\ 0 & 0 & 2\left(2\kappa^2 - \tilde{\alpha}(\kappa)\right) \end{bmatrix},$$

where

$$\tilde{\alpha}(\kappa) = (2\kappa^2 + 1) - \xi^{\mathrm{DW}}(\kappa) e^{\kappa^2}.$$

The corresponding fourth-order orientation tensor,

$$\langle \mathbf{n}^{\otimes 4} \rangle^{\mathrm{DW}}_{\mathbf{m}_3,\kappa} := \int_{S^2} \rho^{\mathrm{DW}}_{\mathbf{m}_3,\kappa}(\mathbf{n}) \mathbf{n}^{\otimes 4} \, d\sigma,$$

has the 6D second-order tensor representation

$$\frac{1}{32\kappa^4} \begin{bmatrix} 3\tilde{a}(\kappa) & \tilde{a}(\kappa) & \tilde{c}(\kappa) & 0 & 0 & 0 \\ \tilde{a}(\kappa) & 3\tilde{a}(\kappa) & \tilde{c}(\kappa) & 0 & 0 & 0 \\ \tilde{c}(\kappa) & \tilde{c}(\kappa) & \tilde{b}(\kappa) & 0 & 0 & 0 \\ 0 & 0 & 0 & 2\tilde{c}(\kappa) & 0 & 0 \\ 0 & 0 & 0 & 0 & 2\tilde{c}(\kappa) & 0 \\ 0 & 0 & 0 & 0 & 0 & 2\tilde{a}(\kappa) \end{bmatrix},$$

where

$$\tilde{a}(\kappa) = 4\kappa^2(\kappa^2+1) + 3 - (2\kappa^2+3)\xi^{\mathrm{DW}}(\kappa)e^{\kappa^2},$$
$$\tilde{b}(\kappa) = 8\left[3 + (2\kappa^2-3)\xi^{\mathrm{DW}}(\kappa)e^{\kappa^2}\right],$$
$$\tilde{c}(\kappa) = 4\left[3\xi^{\mathrm{DW}}(\kappa)e^{\kappa^2} - (2\kappa^2+3)\right].$$

We note that, since the trace of even-order orientation tensors is equal to one, the three functions $\tilde{a}(\cdot)$, $\tilde{b}(\cdot)$ and $\tilde{c}(\cdot)$ satisfy the relation

$$8\tilde{a}(\kappa) + \tilde{b}(\kappa) + 4\tilde{c}(\kappa) = 32\kappa^4.$$

3.3 The Singular-Kernel ODF

The uni-modal ODF with modal vector $\mathbf{m} \in S^2$ and concentration parameter $0 < K < 1$ given by

$$\rho^{\mathrm{SK}}_{\mathbf{m},K}(\mathbf{n}) = \frac{\xi^{\mathrm{SK}}(K)}{4\pi}\frac{1}{1-2K(\mathbf{m}\cdot\mathbf{n})+K^2}, \tag{21}$$

where

$$\xi^{\mathrm{SK}}(K) = \frac{K}{\tanh^{-1}K},$$

is called the singular-kernel distribution [32]. It should be noted that this distribution is not invariant under the inversion of directions: $\mathbf{n} \mapsto -\mathbf{n}$. In Fig. 5 we present plots of (21) for various values of the concentration parameter K.

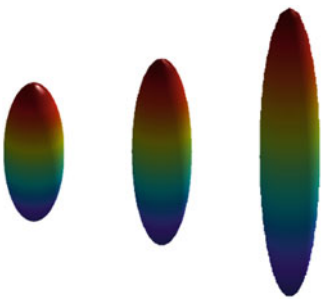

Fig. 5 Plots of the transversely hemitropic ODF (21) for $K = \frac{2}{3}, \frac{3}{4}$, and $\frac{5}{6}$

When $\mathbf{m} = \mathbf{e}_3$, the corresponding first-order orientation tensor is

$$\langle \mathbf{n} \rangle^{\mathrm{SK}}_{\mathbf{m}_3,K} := \int_{S^2} \rho^{\mathrm{SK}}_{\mathbf{m}_3,K}(\mathbf{n})\mathbf{n}\, d\sigma = \frac{1}{2K} \begin{bmatrix} & 0 & \\ & 0 & \\ & K^2 + 1 - \xi^{\mathrm{SK}}(K) & \end{bmatrix},$$

and the corresponding second-order orientation tensor is

$$\langle \mathbf{n}^{\otimes 2} \rangle^{\mathrm{SK}}_{\mathbf{m}_3,K} := \int_{S^2} \rho^{\mathrm{SK}}_{\mathbf{m}_3,K}(\mathbf{n})\mathbf{n}^{\otimes 2}\, d\sigma = \frac{1}{8K^2} \begin{bmatrix} \hat{\alpha}(K) & 0 & 0 \\ 0 & \hat{\alpha}(K) & 0 \\ 0 & 0 & 2(4K^2 - \hat{\alpha}(K)) \end{bmatrix},$$

where

$$\hat{\alpha}(K) = (K^2 + 1)\xi^{\mathrm{SK}}(K) - (K^2 - 1)^2.$$

The corresponding third-order orientation tensor,

$$\langle \mathbf{n}^{\otimes 3} \rangle^{\mathrm{SK}}_{\mathbf{m}_3,K} := \int_{S^2} \rho_{\mathbf{m}_3,K}(\mathbf{n})\mathbf{n}^{\otimes 3}\, d\sigma,$$

has the matrix representation

$$\frac{1}{16K^3} \begin{bmatrix} 0 & 0 & 0 & 0 & \sqrt{2}\hat{\beta}(K) & 0 \\ 0 & 0 & 0 & \sqrt{2}\hat{\beta}(K) & 0 & 0 \\ \hat{\beta}(K) & \hat{\beta}(K) & \hat{\gamma}(K) & 0 & 0 & 0 \end{bmatrix},$$

where

$$\hat{\beta}(K) = (K^4 - \tfrac{2}{3}K^2 + 1)\xi^{\mathrm{SK}}(K) - (K^6 - K^4 - K^2 + 1),$$
$$\hat{\gamma}(K) = 2\left[(K^6 + 3K^4 + 3K^2 + 1) - (K^4 + \tfrac{10}{3}K^2 + 1)\xi^{\mathrm{SK}}(K)\right].$$

Note that as the contraction of $\langle \mathbf{n}^{\otimes 3} \rangle^{\mathrm{SK}}_{\mathbf{m}_3,K}$ is equal to $\langle \mathbf{n} \rangle_{\mathbf{m}_3,K}$ we can verify that

$$2\hat{\beta}(K) + \hat{\gamma}(K) = 8K^2[(K^2 + 1) - \xi^{\mathrm{SK}}(K)].$$

Similarly, the corresponding fourth-order orientation tensor,

$$\langle \mathbf{n}^{\otimes 4} \rangle^{\mathrm{SK}}_{\mathbf{m}_3,K} := \int_{S^2} \rho_{\mathbf{m}_3,K}(\mathbf{n})\mathbf{n}^{\otimes 4}\, d\sigma,$$

has the 6D second-order tensor representation

$$\frac{1}{128K^4}\begin{bmatrix} 3\hat{a}(K) & \hat{a}(K) & \hat{c}(K) & 0 & 0 & 0 \\ \hat{a}(K) & 3\hat{a}(K) & \hat{c}(K) & 0 & 0 & 0 \\ \hat{c}(K) & \hat{c}(K) & \hat{b}(K) & 0 & 0 & 0 \\ 0 & 0 & 0 & 2\hat{c}(K) & 0 & 0 \\ 0 & 0 & 0 & 0 & 2\hat{c}(K) & 0 \\ 0 & 0 & 0 & 0 & 0 & 2\hat{a}(K) \end{bmatrix},$$

where

$$\hat{a}(K) = (K^8 - 4K^6 + 6K^4 - 4K^2 + 1) - (K^6 - \tfrac{11}{3}K^4 - \tfrac{11}{3}K^2 + 1)\xi^{\mathrm{SK}}(K),$$

$$\hat{b}(K) = 8\left[(K^8 + 4K^6 + 6K^4 + 4K^2 + 1) - (K^6 + \tfrac{13}{3}K^4 + \tfrac{13}{3}K^2 + 1)\xi^{\mathrm{SK}}(K)\right],$$

$$\hat{c}(K) = 4\left[(K^6 + \tfrac{1}{3}K^4 + \tfrac{1}{3}K^2 + 1)\xi^{\mathrm{SK}}(K) - (K^4 - 1)^2\right].$$

Because the trace of even-order orientation tensors is equal to one, the three functions $\hat{a}(\cdot)$, $\hat{b}(\cdot)$ and $\hat{c}(\cdot)$ are dependent. Indeed, they satisfy the relation

$$8\hat{a}(K) + \hat{b}(K) + 4\hat{c}(K) = 128K^4.$$

As mentioned before, the singular-kernel orientation distribution function (21) is not antipodally symmetric. Its antipodally symmetric part is given by

$$(\rho^{\mathrm{SK}}_{\mathbf{m},K})^s(\mathbf{n}) = \frac{\xi^{\mathrm{SK}}(K)}{4\pi}\frac{1+K^2}{(1+K^2)^2 - 4K^2(\mathbf{m}\cdot\mathbf{n})^2}, \tag{22}$$

and its antipodally skew-symmetric part is given by

$$(\rho^{\mathrm{SK}}_{\mathbf{m},K})^a(\mathbf{n}) = \frac{\xi^{\mathrm{SK}}(K)}{4\pi}\frac{2K\mathbf{m}\cdot\mathbf{n}}{(1+K^2)^2 - 4K^2(\mathbf{m}\cdot\mathbf{n})^2}. \tag{23}$$

Plots of (22) for various values of the concentration parameter K are given in Fig. 6.

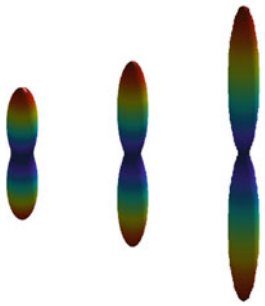

Fig. 6 Plots of the transversely isotropic ODF (22) for $K = \frac{2}{3}, \frac{3}{4}$, and $\frac{5}{6}$

All orientation tensors of even orders relative to the orientation distribution function (22) are equal to the orientation tensors of even orders relative to the orientation distribution function (21), whereas all orientation tensors of odd orders relative to the ODF (22) vanish.

For the comparison with the other distributions, we can compose the functions $\hat{\alpha}(K), \hat{\beta}(K), \hat{\gamma}(K), \hat{a}(K), \hat{b}(K)$, and $\hat{c}(K)$ with the function $K \mapsto \kappa = K/(1+K)$.

3.4 The de la Vallée Poussin ODF

The ODFs

$$\rho^{\mathrm{VP}}_{\mathbf{m},k}(\mathbf{n}) = \frac{2k+1}{4\pi}(\mathbf{n}\cdot\mathbf{m})^{2k}, \tag{24}$$

are a family (indexed by a positive integer k) of antipodally and axially symmetric ODFs. We note here that $\rho^{\mathrm{VP}}_{\mathbf{e}_3,k}(\mathbf{n}) = (\cos\phi)^{2k}$ has the same functional form (with ϕ replaced by $\frac{1}{2}\phi$) as the de la Vallée Poussin distribution in $SO(3)$, the group of rotations in $\mathbb{R}^3$ [26]. Accordingly, we call the family of ODFs (24) the de la Vallée Poussin ODF. The positive integer k acts as the concentration parameter of the Fisher and Watson distributions. Plots of (24) for various values of the concentration parameter k are given in Fig. 7.

For $\rho^{\mathrm{VP}}_{\mathbf{e}_3,k}$, the second-order orientation tensor is

$$\langle \mathbf{n}^{\otimes 2}\rangle^{\mathrm{VP}}_{\mathbf{e}_3,k} := \int_{S^2} \rho^{\mathrm{VP}}_{\mathbf{e}_3,k}(\mathbf{n})\mathbf{n}^{\otimes 2}\, d\sigma = \frac{1}{2k+3}\begin{bmatrix} 1 & 0 & 0 \\ 0 & 1 & 0 \\ 0 & 0 & 2k+1 \end{bmatrix}.$$

The corresponding fourth-order orientation tensor,

$$\langle \mathbf{n}^{\otimes 4}\rangle^{\mathrm{VP}}_{\mathbf{e}_3,k} := \int_{S^2} \rho^{\mathrm{VP}}_{\mathbf{e}_3,k}(\mathbf{n})\mathbf{n}^{\otimes 4}\, d\sigma,$$

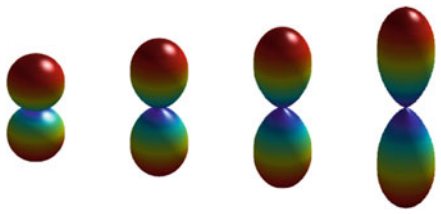

Fig. 7 Plots of the transversely isotropic ODF (24) for $k = 1, 2, 3$ and 5

has the 6D second-order tensor representation

$$\frac{1}{(2k+3)(2k+5)}\begin{bmatrix} 3 & 1 & 2k+1 & 0 & 0 & 0 \\ 1 & 3 & 2k+1 & 0 & 0 & 0 \\ 2k+1 & 2k+1 & (2k+1)(2k+3) & 0 & 0 & 0 \\ 0 & 0 & 0 & 2(2k+1) & 0 & 0 \\ 0 & 0 & 0 & 0 & 2(2k+1) & 0 \\ 0 & 0 & 0 & 0 & 0 & 2 \end{bmatrix}.$$

Using a change of variables we can deduce that the family of ODFs

$$\rho^{\mathrm{VP}}_{\mathbf{e}_1,k}(\mathbf{n}) = \frac{2k+1}{4\pi}\cos^{2k}\theta\sin^{2k}\phi. \tag{25}$$

is transversely isotropic along the $\mathbf{e}_1$-axis. Similarly, the family of ODFs

$$\rho^{\mathrm{VP}}_{\mathbf{e}_2,k}(\mathbf{n}) = \frac{2k+1}{4\pi}\sin^{2k}\theta\sin^{2k}\phi. \tag{26}$$

is transversely isotropic along the $\mathbf{e}_2$-axis.

The de la Vallée Poussin ODF (24) can be generalized as

$$\rho^{\mathrm{VPm}}_{\mathbf{m},\kappa}(\mathbf{n}) = \frac{\kappa+1}{4\pi}|\mathbf{n}\cdot\mathbf{m}|^{\kappa}, \tag{27}$$

where the concentration parameter is now a positive real number κ. The corresponding orientation tensors have the same expressions as the ones for the de la Vallée Poussin ODF, we just need to replace $2k$ with κ.

For all the axially symmetric ODFs discussed in Sect. 3, when the concentration parameter κ is equal to zero, the second- and fourth-order orientation tensors are equal to the isotropic tensors (7) and (8), respectively. On the other hand, when κ goes to infinity, the second- and fourth-order orientation tensors are equal to the totally aligned orientation tensors (11) and (12) with $\mathbf{m} = \mathbf{e}_3$, respectively. For the comparison, in Fig. 8 we present plots of the 11 and 33 components of the second-order orientation tensors, and the 1111 and 3333 components of the fourth-order orientation tensor as functions of the concentration parameter κ and for the different ODFs.

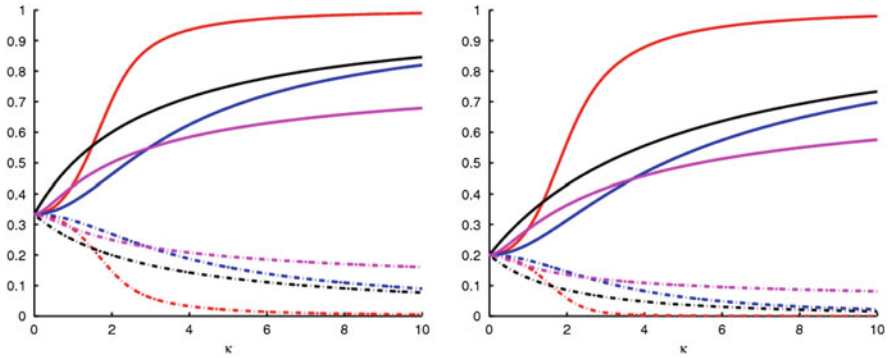

Fig. 8 Plots of the components of the second- and fourth-order orientation tensors as functions of κ for the different ODFs: von Mises-Fisher (*blue*), Watson (*red*), singular kernel (*magenta*), and de la Vallée Poussin (*black*). On the *left* the 11 (*dashed*) and 33 (*solid*) components of the second-order tensor, and on the *right* the 1111 (*dashed*) and 3333 (*solid*) components of the fourth-order tensor

4 Orthotropic ODFs

By adding two transversely isotropic ODFs with the same functional form but different modal vectors we obtain (after multiplication by $\frac{1}{2}$) an orthotropic orientation distribution. For example, by adding $\varrho_{\mathbf{m}^+}$ and $\varrho_{\mathbf{m}^-}$, where $\mathbf{m}^{\pm} = \cos\frac{1}{2}\psi\,\mathbf{e}_1 \pm \sin\frac{1}{2}\psi\,\mathbf{e}_2$, we obtain the orthotropic ODF

$$\varrho^{\text{orth}}(\mathbf{n}) = \tfrac{1}{2}\left(\varrho_{\mathbf{m}^+}(\mathbf{n}) + \varrho_{\mathbf{m}^-}(\mathbf{n})\right). \tag{28}$$

Plots of (28) based on the antipodally symmetric von Mises-Fisher, Watson, antipodally symmetric singular-kernel, and de la Vallée Poussin ODFs with various values of the concentration parameter are given in Fig. 9.

The first- and second-order orientation tensors are given by

$$\langle \mathbf{n} \rangle^{\text{orth}} = \tfrac{1}{2}\begin{bmatrix} 0 \\ 0 \\ A\cos\frac{1}{2}\psi \end{bmatrix}$$

and

$$\langle \mathbf{n}^{\otimes 2} \rangle^{\text{orth}} = \tfrac{1}{2}\begin{bmatrix} 1 - B + (1-3B)\cos\psi & 0 & 0 \\ 0 & 1 - B - (1-3B)\cos\psi & 0 \\ 0 & 0 & 2B \end{bmatrix},$$

where A and B are given in (14) for the chosen ODF $\varrho_{\mathbf{m}}$.

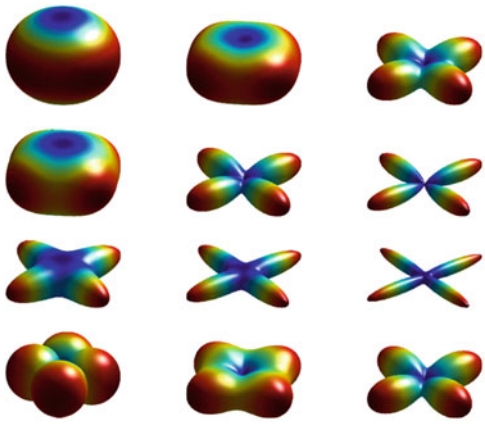

Fig. 9 Plots of orthotropic ODFs based on: antipodally symmetric von Mises-Fisher (*first row*), Watson (*second row*), antipodally symmetric singular kernel (*third row*), and de la Vallée Poussin (*fourth row*)

The third-order orientation tensor has the matrix representation

$$\langle \mathbf{n}^{\otimes 3} \rangle^{\text{orth}} = \tfrac{1}{4} \begin{bmatrix} n_{11} & n_{12} & n_{13} & 0 & 0 & 0 \\ 0 & 0 & 0 & 0 & 0 & \sqrt{2} n_{12} \\ 0 & 0 & 0 & 0 & \sqrt{2} n_{13} & 0 \end{bmatrix},$$

with

$$\begin{aligned} n_{11} &= A(3\cos\tfrac{1}{2}\psi + \cos\tfrac{3}{2}\psi) - C(3\cos\tfrac{1}{2}\psi - 5\cos\tfrac{3}{2}\psi), \\ n_{12} &= A(\cos\tfrac{1}{2}\psi - \cos\tfrac{3}{2}\psi) - C(\cos\tfrac{1}{2}\psi - 5\cos\tfrac{3}{2}\psi), \\ n_{13} &= C\cos\tfrac{1}{2}\psi, \end{aligned}$$

where C is given by (15) for the chosen ODF $\varrho_{\mathbf{m}}$.

The fourth-order orientation tensor has the 6D tensor representation

$$(\mathbf{n}^{\otimes 4})^{\text{orth}} = \begin{bmatrix} N_{11} & N_{12} & N_{13} & 0 & 0 & 0 \\ N_{12} & N_{22} & N_{23} & 0 & 0 & 0 \\ N_{13} & N_{23} & N_{33} & 0 & 0 & 0 \\ 0 & 0 & 0 & 2N_{23} & 0 & 0 \\ 0 & 0 & 0 & 0 & 2N_{13} & 0 \\ 0 & 0 & 0 & 0 & 0 & 2N_{12} \end{bmatrix}$$

with

$$\begin{aligned} N_{11} &= \tfrac{1}{4}(3D + E + 6F) - \tfrac{1}{2}(3D - E)\cos\psi + \tfrac{1}{4}(3D + E - 6F)\cos^2\psi, \\ N_{22} &= \tfrac{1}{4}(3D + E + 6F) + \tfrac{1}{2}(3D - E)\cos\psi + \tfrac{1}{4}(3D + E - 6F)\cos^2\psi, \\ N_{33} &= 3D, \end{aligned}$$

$$N_{12} = \tfrac{1}{2}\left[3D + E - 2F - (3D + E - 6F)\cos^2\psi\right],$$
$$N_{13} = \tfrac{1}{2}\left[D + F - (D - F)\cos\psi\right],$$
$$N_{23} = \tfrac{1}{2}\left[D + F + (D - F)\cos\psi\right],$$

where D, E, and F are given in (16) for the chosen ODF $\varrho_{\mathbf{m}}$.

Other orthotropic ODFs can be obtained by adding two different axially-symmetric ODFs. For example, by adding two axially-symmetric ODFs with orthogonal modal vectors, say $\mathbf{e}_1$ and $\mathbf{e}_2$,

$$\varrho^{1,2}(\mathbf{n}) = \tfrac{1}{2}(\varrho^1_{\mathbf{e}_1}(\mathbf{n}) + \varrho^2_{\mathbf{e}_2}(\mathbf{n})).$$

The corresponding first-order orientation tensor is

$$\langle\mathbf{n}\rangle_{\varrho^{1,2}} := \int_{S^2} \varrho^{1,2}(\mathbf{n})\mathbf{n}\, d\sigma = \tfrac{1}{2}\begin{bmatrix} A_1 \\ A_2 \\ 0 \end{bmatrix},$$

and the corresponding second-order orientation tensor is

$$\langle\mathbf{n}^{\otimes 2}\rangle_{\varrho^{1,2}} := \int_{S^2} \varrho^{1,2}(\mathbf{n})\mathbf{n}^{\otimes 2}\, d\sigma = \tfrac{1}{2}\begin{bmatrix} 1 - B_1 + B_2 & 0 & 0 \\ 0 & 1 + B_1 - B_2 & 0 \\ 0 & 0 & B_1 + B_2 \end{bmatrix},$$

where A_i and B_i are given in (14) for the chosen ODFs $\varrho^i_{\mathbf{e}_i}$, $i = 1, 2$.

The corresponding third-order orientation tensor

$$\langle\mathbf{n}^{\otimes 3}\rangle_{\varrho^{1,2}} := \int_{S^2} \varrho_{\mathbf{e}_3}(\mathbf{n})\mathbf{n}^{\otimes 3}\, d\sigma,$$

has the matrix representation

$$\tfrac{1}{2}\begin{bmatrix} A_1 - 2C_1 & C_1 & C_1 & 0 & 0 & \sqrt{2}C_2 \\ C_2 & A_2 - C_2 & C_2 & 0 & 0 & \sqrt{2}C_1 \\ 0 & 0 & 0 & \sqrt{2}C_2 & \sqrt{2}C_1 & 0 \end{bmatrix},$$

and the corresponding fourth-order orientation tensor,

$$\langle\mathbf{n}^{\otimes 4}\rangle_{\varrho^{1,2}} := \int_{S^2} \varrho^{1,2}(\mathbf{n})\mathbf{n}^{\otimes 4}\, d\sigma,$$

has the 6D second-order tensor representation

$$\frac{1}{2}\begin{bmatrix} E_1+3D_2 & F_1+F_2 & F_1+D_2 & 0 & 0 & 0 \\ F_1+F_2 & 3D_1+E_2 & D_1+F_2 & 0 & 0 & 0 \\ F_1+D_2 & D_1+F_2 & 3(D_1+D_2) & 0 & 0 & 0 \\ 0 & 0 & 0 & 2(D_1+F_2) & 0 & 0 \\ 0 & 0 & 0 & 0 & 2(F_1+D_2) & 0 \\ 0 & 0 & 0 & 0 & 0 & 2(F_1+F_2) \end{bmatrix},$$

where C_i D_i, E_i and F_i are given in (15) and (16) for the chosen ODFs $\varrho^i_{\mathbf{e}_i}$, $i = 1, 2$.

5 Cubic ODFs

By adding three transversely isotropic ODFs with the same functional form and mutually orthogonal modal vectors we obtain (after multiplication by $\frac{1}{3}$) a cubic orientation distribution. For example, by adding $\varrho_{\mathbf{e}_1}$, $\varrho_{\mathbf{e}_2}$ and $\varrho_{\mathbf{e}_3}$, we obtain the cubic orientation distribution

$$\varrho^{\mathrm{cub}}(\mathbf{n}) = \tfrac{1}{3}\left(\varrho_{\mathbf{e}_1}(\mathbf{n}) + \varrho_{\mathbf{e}_2}(\mathbf{n}) + \varrho_{\mathbf{e}_3}(\mathbf{n})\right). \tag{29}$$

Plots of (29) based on the antipodally symmetric von Mises-Fisher, Watson, antipodally symmetric singular kernel, and de la Vallée Poussin ODFs with various values of the concentration parameter are given in Fig. 10.

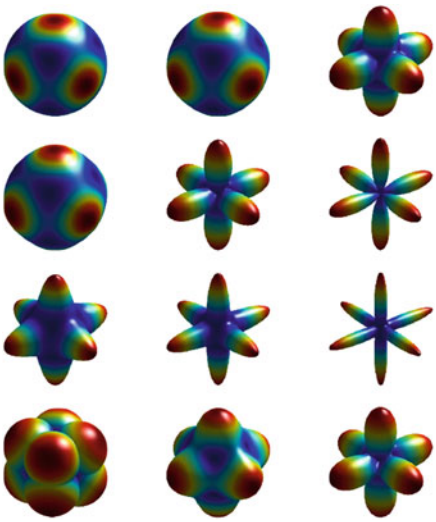

Fig. 10 Plots of cubic ODFs based on: antipodally symmetric von Mises-Fisher (*first row*), Watson (*second row*), antipodally symmetric singular kernel (*third row*), and de la Vallée Poussin (*fourth row*)

The first-order orientation tensor is $\frac{1}{3}A\begin{bmatrix}1 & 1 & 1\end{bmatrix}^T$, where A is given in (14) for the chosen ODF $\varrho_{\mathbf{m}}$. The second-order orientation tensor is equal to $\frac{1}{3}\mathbf{I}$ and the third-order orientation tensor $\langle \mathbf{n}^{\otimes 3}\rangle^{\text{cub}}$ has the matrix representation

$$\frac{1}{3}\begin{bmatrix} A-2C & C & C & 0 & \sqrt{2}C & \sqrt{2}C \\ C & A-2C & C & \sqrt{2}C & 0 & \sqrt{2}C \\ C & C & A-2C & \sqrt{2}C & \sqrt{2}C & 0 \end{bmatrix},$$

where C is given in (15) for the chosen ODF $\varrho_{\mathbf{m}}$.

The fourth-order orientation tensor $\langle \mathbf{n}^{\otimes 4}\rangle^{\text{cub}}$ has the 6D tensor representation

$$\frac{1}{3}\begin{bmatrix} 6D+E & D+2F & D+2F & 0 & 0 & 0 \\ D+2F & 6D+E & D+2F & 0 & 0 & 0 \\ D+2F & D+2F & 6D+E & 0 & 0 & 0 \\ 0 & 0 & 0 & 2(D+2F) & 0 & 0 \\ 0 & 0 & 0 & 0 & 2(D+2F) & 0 \\ 0 & 0 & 0 & 0 & 0 & 2(D+2F) \end{bmatrix},$$

where D, E, and F are given in (16) for the chosen ODF $\varrho_{\mathbf{m}}$.

Another cubic ODF can be obtained by adding four axially symmetric ODFs (with the same functional form)

$$\varrho^{\text{thd}}(\mathbf{n}) = \tfrac{1}{4}\left(\varrho_{\mathbf{a}_1}(\mathbf{n}) + \varrho_{\mathbf{a}_2}(\mathbf{n}) + \varrho_{\mathbf{a}_3}(\mathbf{n}) + \varrho_{\mathbf{a}_4}(\mathbf{n})\right), \tag{30}$$

where

$$\mathbf{a}_1 = \frac{1}{\sqrt{3}}\begin{bmatrix}1\\1\\1\end{bmatrix}, \quad \mathbf{a}_2 = \frac{1}{\sqrt{3}}\begin{bmatrix}1\\-1\\-1\end{bmatrix}, \quad \mathbf{a}_3 = \frac{1}{\sqrt{3}}\begin{bmatrix}-1\\1\\-1\end{bmatrix}, \quad \mathbf{a}_4 = \frac{1}{\sqrt{3}}\begin{bmatrix}-1\\-1\\1\end{bmatrix}.$$

Plots of (30) based on the antipodally symmetric von Mises-Fisher, Watson, antipodally symmetric singular kernel, and de la Vallée Poussin distributions with various values of the concentration parameter are given in Fig. 11. Plots of (30) based on the von Mises-Fisher and singular kernel distributions with various values of the concentration parameter are shown in Fig. 12.

The fact that this ODF has cubic symmetry is not a surprise. Indeed, the tips of the unit vectors $\mathbf{a}_i$, $i = 1, \ldots, 4$ are vertices of a regular tetrahedron. This tetrahedron can be embedded inside the unit cube centered at the origin. Each vertex of the tetrahedron is a vertex of the cube, and each edge of the tetrahedron is a diagonal of one of the cube's faces.

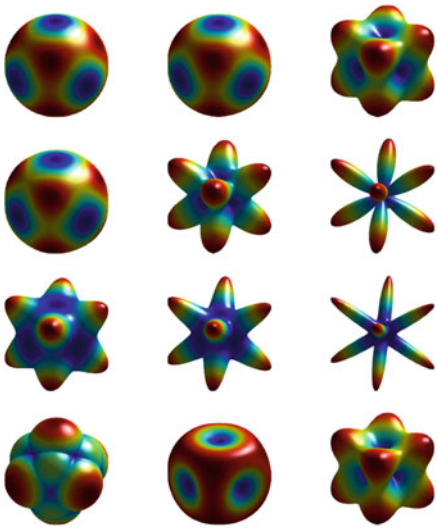

Fig. 11 Plots of tetrahedral ODFs based on: antipodally symmetric von Mises-Fisher (*first row*), Watson (*second row*), antipodally symmetric singular kernel (*third row*), and de la Vallée Poussin (*fourth row*)

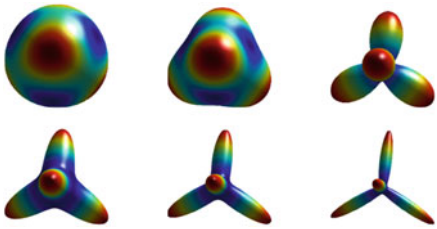

Fig. 12 Plots of tetrahedral ODFs based on: the von Mises-Fisher (*first row*) and the singular kernel (*second row*)

The first-order orientation tensor vanishes and the second-order orientation tensor is equal to $\frac{1}{3}\mathbf{I}$. The third-order orientation tensor has the matrix representation

$$\frac{\sqrt{3}(A-5C)}{9}\begin{bmatrix} 0&0&0&\sqrt{2}&0&0\\ 0&0&0&0&\sqrt{2}&0\\ 0&0&0&0&0&\sqrt{2}\end{bmatrix},$$

while the fourth-order orientation tensor has the 6D tensor representation

$$\frac{1}{9}\begin{bmatrix} 12(D+F)+E & 6D+E & 6D+E & 0 & 0 & 0\\ 6D+E & 12(D+F)+E & 6D+E & 0 & 0 & 0\\ 6D+E & 6D+E & 12(D+F)+E & 0 & 0 & 0\\ 0 & 0 & 0 & 2(6D+E) & 0 & 0\\ 0 & 0 & 0 & 0 & 2(6D+E) & 0\\ 0 & 0 & 0 & 0 & 0 & 2(6D+E)\end{bmatrix},$$

where D, E, and F are given in (16) for the chosen ODF $\varrho_{\mathbf{m}}$.

6 Hexagonal ODFs

By adding three transversely isotropic ODFs (having the same functional form) with planar modal vectors of mutual angles equal to $\frac{2}{3}\pi$ we obtain (after multiplication by $\frac{1}{3}$) a cubic orientation distribution. For example, by adding $\varrho_{\mathbf{e}_1}$, $\varrho_{\mathbf{m}_1}$ and $\varrho_{\mathbf{m}_2}$, where $\mathbf{m}_{1,2} = \frac{1}{2}(-\mathbf{e}_1 \pm \sqrt{3}\mathbf{e}_2)$, we obtain the hexagonal orientation distribution

$$\varrho^{\text{hex}}(\mathbf{n}) = \tfrac{1}{3}\left(\varrho_{\mathbf{e}_1}(\mathbf{n}) + \varrho_{\mathbf{m}_1}(\mathbf{n}) + \varrho_{\mathbf{m}_2}(\mathbf{n})\right). \tag{31}$$

Plots of (31) based on the antipodally symmetric von Mises-Fisher, Watson, antipodally symmetric singular kernel, and de la Vallée Poussin ODFs with various values of the concentration parameter are given in Fig. 13. Plots of (31) based on the von Mises-Fisher and singular-kernel ODFs with various values of the concentration parameter are shown in Fig. 14.

The first-order orientation tensor is $\frac{2}{3}\begin{bmatrix} A & 0 & 0 \end{bmatrix}^T$ and the second-order orientation tensor is

$$\langle \mathbf{n}^{\otimes 2} \rangle^{\text{hex}} = \frac{1}{2}\begin{bmatrix} 1-B & 0 & 0 \\ 0 & 1-B & 0 \\ 0 & 0 & 2B \end{bmatrix},$$

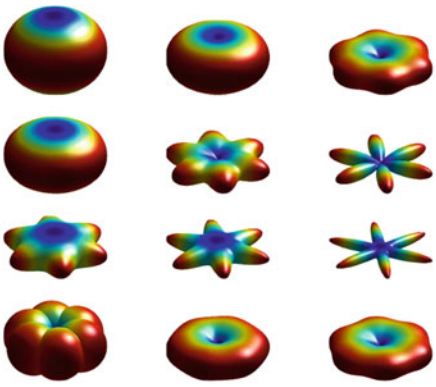

Fig. 13 Plots of hexagonal ODFs based on: antipodally symmetric von Mises-Fisher (*first row*), Watson (*second row*), antipodally symmetric singular kernel (*third row*), and de la Vallée Poussin (*fourth row*)

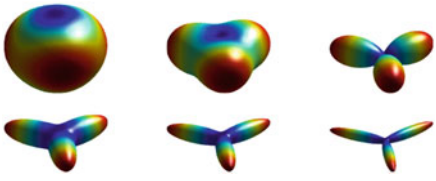

Fig. 14 Plots of hexagonal ODFs based on: the von Mises-Fisher (*first row*) and the singular kernel (*second row*)

where A and B are given in (14) for the chosen ODF $\varrho_{\mathbf{m}}$.

The third-order orientation tensor $\langle \mathbf{n}^{\otimes 3} \rangle^{\text{hex}}$ has the matrix representation

$$\frac{1}{12}\begin{bmatrix} 5A-C & 3A-7C & 8C & 0 & 0 & 0 \\ 0 & 0 & 0 & 0 & 0 & \sqrt{2}(3A-7C) \\ 0 & 0 & 0 & 0 & 8\sqrt{2}C & 0 \end{bmatrix},$$

and the fourth-order orientation tensor $\langle \mathbf{n}^{\otimes 4} \rangle^{\text{hex}}$ has the 6D matrix representation

$$\frac{1}{8}\begin{bmatrix} 3(3D+E+2F) & 3D+E+2F & 4(D+F) & 0 & 0 & 0 \\ 3D+E+2F & 3(3D+E+2F) & 4(D+F) & 0 & 0 & 0 \\ 4(D+F) & 4(D+F) & 24D & 0 & 0 & 0 \\ 0 & 0 & 0 & 8(D+F) & 0 & 0 \\ 0 & 0 & 0 & 0 & 8(D+F) & 0 \\ 0 & 0 & 0 & 0 & 0 & 2(3D+E+2F) \end{bmatrix},$$

where C, D, E, and F are given in (15) and (16) for the chosen ODF $\varrho_{\mathbf{m}}$.

7 Icosahedral ODFs

We have used (elementary) axially symmetric ODFs to construct new ODFs with different material symmetry classes. The eight symmetry classes of fourth-order tensors (isotropy, cubic, orthogonal, hexagonal, tetragonal, trigonal, monoclinic, and triclinic) can thus be obtained. There are more elaborate symmetries that can be detected only in higher order tensors. For example, the cubic symmetry is not detected at the second-order level. Furthermore, the following example exhibits a case where the second- and fourth-order orientation tensors are isotropic whereas the ODF is obviously not. Let $\mathbf{b}_i$, $i = 1, \ldots, 6$ be the unit vectors pointing to the opposite vertices of a regular icosahedron and given by

$$\mathbf{b}_{1,2} = \frac{1}{\sqrt{1+\tau^2}}\begin{bmatrix} 0 \\ 1 \\ \pm\tau \end{bmatrix}, \quad \mathbf{b}_{3,4} = \frac{1}{\sqrt{1+\tau^2}}\begin{bmatrix} \pm\tau \\ 0 \\ 1 \end{bmatrix}, \quad \mathbf{b}_{5,6} = \frac{1}{\sqrt{1+\tau^2}}\begin{bmatrix} 1 \\ \pm\tau \\ 0 \end{bmatrix},$$

where $\tau = (1+\sqrt{5})/2$. Let us consider the ODF obtained by adding the six axially symmetric ODFs with modal vectors $\mathbf{b}_i$:

$$\varrho^{\text{ico}}(\mathbf{n}) = \tfrac{1}{6}\left(\varrho_{\mathbf{b}_1}(\mathbf{n}) + \varrho_{\mathbf{b}_2}(\mathbf{n}) + \varrho_{\mathbf{b}_3}(\mathbf{n}) + \varrho_{\mathbf{b}_4}(\mathbf{n}) + \varrho_{\mathbf{b}_5}(\mathbf{n}) + \varrho_{\mathbf{b}_6}(\mathbf{n})\right). \tag{32}$$

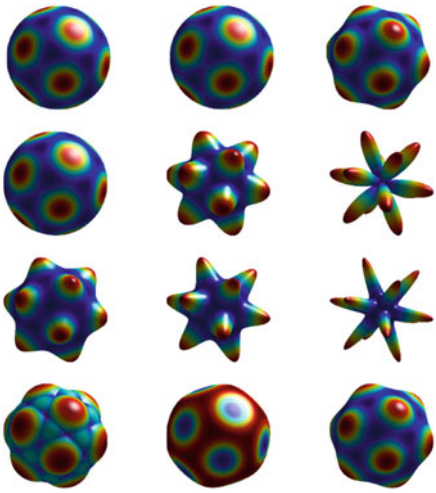

Fig. 15 Plots of icosahedral ODFs based on: antipodally symmetric von Mises-Fisher (*first row*), Watson (*second row*), antipodally symmetric singular kernel (*third row*), and de la Vallée Poussin (*fourth row*)

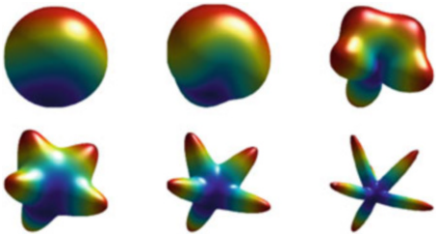

Fig. 16 Plots of icosahedral ODFs based on: the von Mises-Fisher (*first row*) and the singular kernel (*second row*)

Plots of (32) based on the antipodally symmetric von Mises-Fisher, Watson, antipodally symmetric singular-kernel, and de la Vallée Poussin ODFs with various values of the concentration parameter are given in Fig. 15. Plots of (32) based on the von Mises-Fisher and singular kernel ODFs with various values of the concentration parameter are shown in Fig. 16.

The first-order orientation tensor is equal to $A/(3\sqrt{1+\tau^2})\,[1\ 1\ 1]^T$, where A is given in (14) for the chosen ODF $\varrho_{\mathbf{m}}$. The second- and fourth-order orientation tensors are the isotropic tensors (7) and (8), respectively. The third-order orientation tensor has the representation

$$\frac{\sqrt{5}\tau}{30\sqrt{1+\tau^2}}\begin{bmatrix} u & v & w & 0 & \sqrt{2}v & \sqrt{2}w \\ w & u & v & \sqrt{2}w & 0 & \sqrt{2}v \\ v & w & u & \sqrt{2}v & \sqrt{2}w & 0 \end{bmatrix},$$

with

$$u = (3-\sqrt{5})A + 2\sqrt{5}C, \quad v = 2A - \sqrt{5}(\sqrt{5}+1)C, \quad w = \sqrt{5}(\sqrt{5}-1)C,$$

where C is given in (15) for the chosen ODF $\varrho_{\mathbf{m}}$.

8 General ODFs

As we have seen, in many cases it suffices to look at approximations (3) or (4) up to the order four. However, certain ODFs cannot be approximated by only keeping low-order terms and one has to consider higher-order approximations. Moreover, empirically, we may wish to measure or estimate a fiber ODF or its moments, so a convenient and general representation in terms of a complete and orthogonal set of basis functions is sought.

We claim that any ODF can be approximated by a sum of axially symmetric ODFs with different modal vectors and concentration parameters. For instance, one can use the uni-modal de la Vallée Poussin ODF as its related tensors are easily computed. In fact, the de la Vallée Poussin can be expressed in terms of the Cartesian coordinates as

$$\rho^{\mathrm{VP}}_{\mathbf{m},k}(\mathbf{n}) = R_{\mathbf{m},k}(x,y,z) := (m_1 x + m_2 y + m_3 z)^{2k} = (\mathbf{m}\cdot\mathbf{n})^{2k},$$

where, of course, the coordinates x, y, and z of $\mathbf{n}$ are constrained to satisfy the condition $x^2 + y^2 + z^2 = 1$.

Therefore, any square-integrable function on S^2 can be approximated by

$$f(\mathbf{n}) \sim \sum_{k=0}^{K}\sum_{l=1}^{L} f_{kl}\, R_{\mathbf{m}_l,k}(\mathbf{n}),$$

where $\mathbf{m}_l$ are unit vectors. For the determination of this (simple) approximation one can seek, for given K and L, unit vectors $\mathbf{m}_l$ and coefficients $f_{k,l}$ minimizers of the functional

$$\int_{S^2}\left[f(\mathbf{n}) - \sum_{k=1}^{K}\sum_{l=1}^{L} f_{k,l}(\mathbf{m}_l\cdot\mathbf{n})^{2k}\right]^2 d\sigma.$$

If we take only one value of the concentration parameter (power) in the de la Vallée Poussin kernel in the above approximation, i.e., we assume $f_{k,l} = 0$ for all $k < K$, then the above minimization problem reduces to finding unit vectors $\mathbf{m}_l$ and coefficients $\tilde{f}_l$ minimizers of the functional

$$\int_{S^2}\left[f(\mathbf{n}) - \sum_{l=1}^{L} \tilde{f}_l(\mathbf{m}_l\cdot\mathbf{n})^{2K}\right]^2 d\sigma.$$

This minimization problem is similar to the low-rank approximation approach of Schultz and Seidel [27] for estimating crossing fibers from an ODF generated by Q-ball imaging or spherical deconvolution. When the ODF is also estimated from diffusion weighed imaging signals, Gur et al. [13] presented a nonlinear

method for the joint estimation of the ODF, extracting the fiber directions using low-rank approximations. We also mention that Ghosh et al. [11] and Megherbi et al. [20] used similar techniques for extracting fiber directions without any prior information about the number of fibers. These works employ the symmetric tensor decomposition algorithm proposed in [4] which is based on the decomposition of homogeneous polynomials as a sum of powers of linear forms.

Alternatively, if the coefficients of the expansion in spherical harmonics of the ODF are given (estimated from experimental data or computed from a given ODF), then one can compute the orientation tensors explicitly as shown below. Recall that any ODF can be expanded in real spherical harmonics

$$\rho(\mathbf{n}) = \sum_{l=0}^{\infty} \sum_{m=-l}^{l} c_{l,m} S_{l,m}(\theta, \phi).$$

Here $S_{l,m}(\cdot,\cdot)$ are the (normalized) real spherical harmonics of degree l and order m defined by

$$S_{l,m}(\theta,\phi) = \begin{cases} \frac{(-1)^m}{\sqrt{2}}(Y_{l,m}(\theta,\phi) + \bar{Y}_{l,m}(\theta,\phi)) & \text{for } m > 0, \\ Y_{l,0}(\theta,\phi) & \text{for } m = 0, \\ \frac{(-1)^m}{i\sqrt{2}}(Y_{l,-m}(\theta,\phi) - \bar{Y}_{l,-m}(\theta,\phi)) & \text{for } m < 0, \end{cases}$$

where the complex spherical harmonics $Y_{l,m}(\cdot,\cdot)$ (and its complex conjugate $\bar{Y}_{m,l}(\cdot,\cdot)$) are related to the associated Legendre polynomials $P_l^m(\cdot)$ by

$$Y_{l,m}(\theta,\phi) = (-1)^m \sqrt{\frac{2l+1}{4\pi}\frac{(m-l)!}{(m+l)!}} P_l^m(\cos\theta)\exp(im\phi).$$

For example, the non-vanishing spherical harmonic coefficients up to the order four for the von Mises-Fisher ODF (17) are

$$c_{0,0} = \frac{1}{2\sqrt{\pi}}, \quad c_{1,0} = \frac{\sqrt{3}\,(\kappa\cosh\kappa - \sinh\kappa)}{2\sqrt{\pi}\kappa\sinh\kappa},$$

$$c_{2,0} = \frac{\sqrt{5}\left((3+\kappa^2)\sinh\kappa - 3\kappa\cosh\kappa\right)}{2\sqrt{\pi}\kappa^2\sinh\kappa},$$

$$c_{3,0} = \frac{\sqrt{7}\left(\kappa(\kappa^2+15)\cosh\kappa - 3(2\kappa^2+5)\sinh\kappa\right)}{2\sqrt{\pi}\kappa^3\sinh\kappa},$$

$$c_{4,0} = \frac{3\left((\kappa^4+45\kappa^2+105)\sinh\kappa - 5\kappa(2\kappa^2+21)\cosh\kappa\right)}{2\sqrt{\pi}\kappa^4\sinh\kappa}.$$

Similarly, the non-vanishing spherical harmonic coefficients up to order four for the Watson ODF (20) are

$$c_{0,0} = \frac{1}{2\sqrt{\pi}}, \quad c_{2,0} = \frac{\sqrt{5}\left(6\kappa e^{\kappa^2} - \sqrt{\pi}(2\kappa^2+3)\operatorname{erfi}\kappa\right)}{8\pi\kappa^2\operatorname{erfi}\kappa},$$

$$c_{4,0} = \frac{3\left(10\kappa(2\kappa^2-21)e^{\kappa^2} + 3\sqrt{\pi}(4\kappa^4+20\kappa^2+35)\operatorname{erfi}\kappa\right)}{64\pi\kappa^4\operatorname{erfi}\kappa}.$$

When the spherical harmonic coefficients $c_{l,m}$, $l = 0, \ldots, 4, m = -l, \ldots l$, of an ODF ρ are given then we can compute the orientation tensors up to order four. The first-order orientation tensor is

$$\langle \mathbf{n} \rangle_\rho = 2\sqrt{\frac{\pi}{3}} \sum_{m=-1}^{1} c_{1,m}\mathbf{s}^{1,m}, \tag{33}$$

the second-order orientation tensor is

$$\langle \mathbf{n}^{\otimes 2} \rangle_\rho = 2\sqrt{\frac{\pi}{3}} \left(c_{0,0}\mathbf{S}^{0,0} + \sqrt{\frac{2}{5}} \sum_{m=-2}^{2} c_{2,m}\mathbf{S}^{2,m} \right), \tag{34}$$

the third-order orientation tensor is

$$\langle \mathbf{n}^{\otimes 3} \rangle_\rho = 2\sqrt{\frac{\pi}{5}} \left(\sum_{m=-1}^{1} c_{1,m}\mathsf{S}^{1,m} + \sqrt{\frac{2}{7}} \sum_{m=-3}^{3} c_{3,m}\mathsf{S}^{3,m} \right), \tag{35}$$

and the fourth-order orientation tensor is

$$\langle \mathbf{n}^{\otimes 4} \rangle_\rho = 2\sqrt{\frac{\pi}{3}} \left(c_{0,0}\mathbb{S}^{0,0} + \sqrt{\frac{2}{5}} \sum_{m=-2}^{2} c_{2,m}\mathbb{S}^{2,m} + \frac{2}{\sqrt{105}} \sum_{m=-4}^{4} c_{4,m}\mathbb{S}^{4,m} \right). \tag{36}$$

The vectors $\mathbf{s}^{l,m}$, second-order tensors $\mathbf{S}^{l,m}$, third-order tensors $\mathsf{S}^{l,m}$ and fourth-order tensors $\mathbb{S}^{l,m}$ are given in the Appendix.

9 Discussion and Concluding Remarks

We have presented explicit expressions of the orientation tensors up to order four for a hierarchy of ODFs with different material symmetries. We have given the coefficients of these orientation tensors in a natural coordinate system. However, we recognize that to use these ODF with experimental data, the mean direction

vector may also need to be included in these distributions as a random variable and estimated. We have seen that by combining axially symmetric ODFs with different modal vectors and concentration parameters one can get an ODF with more complex material symmetry. Inversely, we claim that a given ODF can be well approximated by a convex combination of axially symmetric ones. However, finding such an approximation can be complicated due to non-uniqueness. Alternatively, we proposed using the approximation of this ODF by spherical harmonics up to a specified order. For each order, the orientation tensors are given by a linear combination of pre-computed tensors that form an orthonormal basis.

If from experimental data we can estimate the coefficients of the expansion in spherical harmonics of the ODF, then by using this framework we can compute the orientation tensors. From the orientation tensors we can infer the material symmetries (or direction of the fibers) by the method developed in [5].

Appendix

We give here the expressions for the normalized orientation-like tensors that appear in (33)–(36).

The vectors $\mathbf{s}^{1,m}$, $m = -1, \ldots, 1$, which are obtained from $\int_{S^2} S^{1,m}(\theta,\phi)\mathbf{n}\, d\sigma$ by normalization, are given by

$$\mathbf{s}^{1,-1} = \begin{bmatrix} -1 \\ 0 \\ 0 \end{bmatrix}, \quad \mathbf{s}^{1,0} = \begin{bmatrix} 0 \\ 0 \\ 1 \end{bmatrix}, \quad \mathbf{s}^{1,1} = \begin{bmatrix} 0 \\ -1 \\ 0 \end{bmatrix}.$$

The second-order tensors $\mathbf{S}^{l,m}$, $l = 0, 2$, $m = -l, \ldots, l$, which are obtained from $\int_{S^2} S^{l,m}(\theta,\phi)\mathbf{n}^{\otimes 2}\, d\sigma$ by normalization, are given by

$$\mathbf{S}^{0,0} = \frac{1}{\sqrt{3}}\begin{bmatrix} 1 & 0 & 0 \\ 0 & 1 & 0 \\ 0 & 0 & 1 \end{bmatrix}, \quad \mathbf{S}^{2,-2} = \frac{1}{\sqrt{2}}\begin{bmatrix} 1 & 0 & 0 \\ 0 & -1 & 0 \\ 0 & 0 & 0 \end{bmatrix}, \quad \mathbf{S}^{2,-1} = \frac{1}{\sqrt{2}}\begin{bmatrix} 0 & 0 & -1 \\ 0 & 0 & 0 \\ -1 & 0 & 0 \end{bmatrix},$$

$$\mathbf{S}^{2,0} = \frac{1}{\sqrt{6}}\begin{bmatrix} -1 & 0 & 0 \\ 0 & -1 & 0 \\ 0 & 0 & 2 \end{bmatrix}, \quad \mathbf{S}^{2,1} = \frac{1}{\sqrt{2}}\begin{bmatrix} 0 & 0 & 0 \\ 0 & 0 & -1 \\ 0 & -1 & 0 \end{bmatrix}, \quad \mathbf{S}^{2,2} = \frac{1}{\sqrt{2}}\begin{bmatrix} 0 & 1 & 0 \\ 1 & 0 & 0 \\ 0 & 0 & 0 \end{bmatrix}.$$

Note that $\mathbf{S}^{l,m}$ are traceless except for $\mathbf{S}^{0,0}$ which has unit trace. Furthermore, the set $\{\mathbf{S}^{l,m},\ l = 0, 2,\ m = -l, \ldots, l\}$ forms an orthonormal basis of the space of symmetric second-order tensors.

The third-order tensors $\mathsf{S}^{l,m}$, $l = 1, 3$, $m = -l, \ldots, l$, which are obtained from $\int_{S^2} S^{l,m}(\theta,\phi)\mathbf{n}^{\otimes 3}\, d\sigma$ by normalization, are given by

$$\mathsf{S}^{1,-1} = \frac{1}{\sqrt{15}}\begin{bmatrix} -3 & -1 & -1 & 0 & 0 & 0 \\ 0 & 0 & 0 & 0 & 0 & -\sqrt{2} \\ 0 & 0 & 0 & 0 & -\sqrt{2} & 0 \end{bmatrix}, \quad \mathsf{S}^{1,0} = \frac{1}{\sqrt{15}}\begin{bmatrix} 0 & 0 & 0 & 0 & \sqrt{2} & 0 \\ 0 & 0 & 0 & \sqrt{2} & 0 & 0 \\ 1 & 1 & 3 & 0 & 0 & 0 \end{bmatrix}, \quad \mathsf{S}^{1,1} = \frac{1}{\sqrt{15}}\begin{bmatrix} 0 & 0 & 0 & 0 & 0 & -\sqrt{2} \\ -1 & -3 & -1 & 0 & 0 & 0 \\ 0 & 0 & 0 & -\sqrt{2} & 0 & 0 \end{bmatrix},$$

$$\mathsf{S}^{3,-3}=\frac{1}{2}\begin{bmatrix}-1&1&0&0&0&0\\0&0&0&0&0&\sqrt{2}\\0&0&0&0&0&0\end{bmatrix},\quad \mathsf{S}^{3,-2}=\frac{1}{\sqrt{6}}\begin{bmatrix}0&0&0&0&\sqrt{2}&0\\0&0&0&-\sqrt{2}&0&0\\1&-1&0&0&0&0\end{bmatrix},\quad \mathsf{S}^{3,-1}=\frac{1}{2\sqrt{15}}\begin{bmatrix}3&3&-4&0&0&0\\0&0&0&0&0&\sqrt{2}\\0&0&0&0&-4\sqrt{2}&0\end{bmatrix},$$

$$\mathsf{S}^{3,0}=\frac{1}{\sqrt{10}}\begin{bmatrix}0&0&0&0&-\sqrt{2}&0\\0&0&0&-\sqrt{2}&0&0\\-1&-1&2&0&0&0\end{bmatrix},\quad \mathsf{S}^{3,1}=\frac{1}{2\sqrt{15}}\begin{bmatrix}0&0&0&0&0&\sqrt{2}\\1&1&-4&0&0&0\\0&0&0&-4\sqrt{2}&0&0\end{bmatrix},\quad \mathsf{S}^{3,2}=\frac{1}{\sqrt{6}}\begin{bmatrix}0&0&0&\sqrt{2}&0&0\\0&0&0&0&\sqrt{2}&0\\0&0&0&0&0&\sqrt{2}\end{bmatrix},$$

$$\mathsf{S}^{3,3}=\frac{1}{2}\begin{bmatrix}0&0&0&0&0&-\sqrt{2}\\-1&1&0&0&0&0\\0&0&0&0&0&0\end{bmatrix}.$$

We remark that the set $\{\mathsf{S}^{l,m},\ l=1,3,\ m=-l,\ldots,l\}$ forms an orthonormal basis of the space of totally symmetric third-order tensors.

The fourth-order tensors $\mathbb{S}^{l,m}$, $l=0,2,4$, $m=-l,\ldots,l$, which are obtained from $\int_{S^2} S^{l,m}(\theta,\phi)\mathbf{n}^{\otimes 4}\,d\sigma$ by normalization, are given by

$$\mathbb{S}^{0,0}=\frac{1}{3\sqrt{5}}\begin{bmatrix}3&1&1&0&0&0\\1&3&1&0&0&0\\1&1&3&0&0&0\\0&0&0&2&0&0\\0&0&0&0&2&0\\0&0&0&0&0&2\end{bmatrix},\quad \mathbb{S}^{2,-2}=\frac{1}{2\sqrt{21}}\begin{bmatrix}6&0&1&0&0&0\\0&-6&-1&0&0&0\\1&-1&0&0&0&0\\0&0&0&-2&0&0\\0&0&0&0&2&0\\0&0&0&0&0&0\end{bmatrix},\quad \mathbb{S}^{2,-1}=\frac{1}{2\sqrt{21}}\begin{bmatrix}0&0&0&0&-3\sqrt{2}&0\\0&0&0&0&-\sqrt{2}&0\\0&0&0&0&-3\sqrt{2}&0\\0&0&0&0&0&-2\\-3\sqrt{2}&-\sqrt{2}&-3\sqrt{2}&0&0&0\\0&0&0&-2&0&0\end{bmatrix},$$

$$\mathbb{S}^{2,0}=\frac{1}{2\sqrt{63}}\begin{bmatrix}-6&-2&1&0&0&0\\-2&-6&1&0&0&0\\1&1&12&0&0&0\\0&0&0&2&0&0\\0&0&0&0&2&0\\0&0&0&0&0&-4\end{bmatrix},\quad \mathbb{S}^{2,1}=\frac{1}{2\sqrt{21}}\begin{bmatrix}0&0&0&-\sqrt{2}&0&0\\0&0&0&-3\sqrt{2}&0&0\\0&0&0&-3\sqrt{2}&0&0\\-\sqrt{2}&-3\sqrt{2}&-3\sqrt{2}&0&0&0\\0&0&0&0&0&-2\\0&0&0&0&-2&0\end{bmatrix},\quad \mathbb{S}^{2,2}=\frac{1}{2\sqrt{21}}\begin{bmatrix}0&0&0&0&3\sqrt{2}\\0&0&0&0&3\sqrt{2}\\0&0&0&0&\sqrt{2}\\0&0&0&2&0\\0&0&0&2&0\\3\sqrt{2}&3\sqrt{2}&\sqrt{2}&0&0&0\end{bmatrix},$$

$$\mathbb{S}^{4,-4}=\frac{1}{2\sqrt{2}}\begin{bmatrix}1&-1&0&0&0&0\\-1&1&0&0&0&0\\0&0&0&0&0&0\\0&0&0&0&0&0\\0&0&0&0&0&0\\0&0&0&0&0&-2\end{bmatrix},\quad \mathbb{S}^{4,-3}=\frac{1}{4}\begin{bmatrix}0&0&0&0&-\sqrt{2}&0\\0&0&0&0&\sqrt{2}&0\\0&0&0&0&0&0\\0&0&0&0&0&2\\-\sqrt{2}&\sqrt{2}&0&0&0&0\\0&0&0&2&0&0\end{bmatrix},\quad \mathbb{S}^{4,-2}=\frac{1}{\sqrt{14}}\begin{bmatrix}-1&0&1&0&0&0\\0&1&-1&0&0&0\\1&-1&0&0&0&0\\0&0&0&-2&0&0\\0&0&0&0&2&0\\0&0&0&0&0&0\end{bmatrix},$$

$$\mathbb{S}^{4,-1}=\frac{1}{\sqrt{28}}\begin{bmatrix}0&0&0&0&3\sqrt{2}&0\\0&0&0&0&\sqrt{2}&0\\0&0&0&0&-4\sqrt{2}&0\\0&0&0&0&0&2\\3\sqrt{2}&\sqrt{2}&-4\sqrt{2}&0&0&0\\0&0&0&2&0&0\end{bmatrix},\quad \mathbb{S}^{4,0}=\frac{1}{2\sqrt{70}}\begin{bmatrix}3&1&-4&0&0&0\\1&3&-4&0&0&0\\-4&-4&8&0&0&0\\0&0&0&-8&0&0\\0&0&0&0&-8&0\\0&0&0&0&0&2\end{bmatrix},\quad \mathbb{S}^{4,1}=\frac{1}{2\sqrt{28}}\begin{bmatrix}0&0&0&\sqrt{2}&0&0\\0&0&0&3\sqrt{2}&0&0\\0&0&0&-4\sqrt{2}&0&0\\\sqrt{2}&3\sqrt{2}&-4\sqrt{2}&0&0&0\\0&0&0&0&0&2\\0&0&0&0&2&0\end{bmatrix},$$

$$\mathbb{S}^{4,2}=\frac{1}{2\sqrt{14}}\begin{bmatrix}0&0&0&0&0&-\sqrt{2}\\0&0&0&0&0&-\sqrt{2}\\0&0&0&0&0&2\sqrt{2}\\0&0&0&0&4&0\\0&0&0&4&0&0\\-\sqrt{2}&-\sqrt{2}&2\sqrt{2}&0&0&0\end{bmatrix},\quad \mathbb{S}^{4,3}=\frac{1}{4}\begin{bmatrix}0&0&0&-\sqrt{2}&0&0\\0&0&0&\sqrt{2}&0&0\\0&0&0&0&0&0\\-\sqrt{2}&\sqrt{2}&0&0&0&0\\0&0&0&0&0&-2\\0&0&0&0&-2&0\end{bmatrix},\quad \mathbb{S}^{4,4}=\frac{1}{2\sqrt{2}}\begin{bmatrix}0&0&0&0&\sqrt{2}\\0&0&0&0&-\sqrt{2}\\0&0&0&0&0\\0&0&0&0&0\\0&0&0&0&0\\\sqrt{2}&-\sqrt{2}&0&0&0&0\end{bmatrix}.$$

It should be noted that $\mathbb{S}^{l,m}$ are traceless except for $\mathbb{S}^{0,0}$ which has unit trace. The set $\{\mathbb{S}^{l,m},\ l=0,2,4,\ m=-l,\ldots,l\}$ forms an orthonormal basis of the space of totally symmetric fourth-order tensors.

References

1. Advani, S.G., Tucker III, C.L.: The use of tensors to describe and predict fiber orientation in short fiber composites. J. Rheol. **31**(8), 751–784 (1987)
2. Advani, S.G., Tucker III, C.L.: Closure approximations for three-dimensional structure tensors. J. Rheol. **34**(3), 367–386 (1990)
3. Backus, G.: A geometric picture of anisotropic elastic tensors. Rev. Geophys. Space Phys. **8**(3), 633–671 (1970)
4. Brachat, J., Comon, P., Mourrain, B., Tsigaridas, E.P.: Symmetric tensor decomposition. Linear Algebra Appl. **433**(11–12), 1851–1872 (2010)
5. Chebbi, Z.: Study of brain white matter fiber crossings using fourth-order diffusion tensors estimated from HARDI data. Master's thesis, National Engineering School at Tunis (2009)
6. Cieslinski, M.M., Steel, P.J., Lincoln, S.F., Easton, C.J.: Centrosymmetric and non-centrosymmetric packing of aligned molecular fibers in the solid state self assemblies of cyclodextrin-based rotaxanes. Supramol. Chem. **18**, 529–536 (2006)
7. Eberlea, A.P.R., Vélez-Garcíab, G.M., Bairda, D.G., Wapperomc P.: Fiber orientation kinetics of a concentrated short glass fiber suspension in startup of simple shear flow. J. Non-Newtonian Fluid Mech. **165**, 110–119 (2010)
8. Fisher, N.I., Lewis, T., Embleton, B.J.J.: Statistical Analysis of Spherical Data. Cambridge University Press, Cambridge (1987)
9. Florack, L., Balmashnova, E.: Two canonical representations for regularized high angular resolution diffusion imaging. In: Alexander, D., Gee, J., Whitaker, R. (eds.) MICCAI Workshop on Computational Diffusion MRI, New York, pp. 85–96 (2008)
10. Florack, L., Balmashnova, E., Astola, L., Brunenberg, E.: A new tensorial framework for single-shell high angular resolution diffusion imaging. J. Math. Imaging Vision **38**(3), 171–181 (2010)
11. Ghosh, A., Megherbi, T., Oulebsir-Boumghar, F., Deriche, R.: Fiber orientation distribution from non-negative sparse recovery. In: IEEE 10th International Symposium on Biomedical Imaging (ISBI), 2013, pp. 254–257 (2013)
12. Goldacker, T., Abetz, V., Stadler, R., Erukhimovich, I., Leibler, L.: Non-centrosymmetric superlattices in block copolymer blends. Nature **398**, 137–139 (1999)
13. Gur, Y., Jiao, F., Zhu, S.X., Johnson, C.R.: White matter structure assessment from reduced HARDI data using low-rank polynomial approximations. In: Panagiotaki, E., O'Donnell, L., Schultz, T., Zhang, G.H. (eds.) Proceedings of the Computational Diffusion MRI, pp. 186–197 (2012)
14. Jack, D.A., Smith, D.E.: Elastic properties of short-fiber polymer composites, derivation and demonstration of analytical forms for expectation and variance from orientation tensors. J. Compos. Mater. **42**(3), 277–308 (2008)
15. Jones, M.N.: Spherical Harmonics and Tensors for Classical Field Theory. Wiley, New York (1985)
16. Kanatani, K.-I.: Distribution of directional data and fabric tensors. Int. J. Eng. Sci. **22**(2), 149–164 (1984)
17. Lakes, R.: Elastic and viscoelastic behavior of chiral materials. Int. J. Mech. Sci. **43**(7), 1579–1589 (2001)
18. Liu, C., Bammer, R., Acar, B., Moseley, M.E.: Characterizing non-gaussian diffusion by using generalized diffusion tensors. Magn. Reson. Med. **51**, 924–937 (2004)
19. Mardia, K.V.: Statistics of directional data. J. R. Stat. Soc. Ser. B **37**(3), 349–393 (1975)
20. Megherbi, T., Kachouane, M., Oulebsir-Boumghar, F., Deriche, R.: Crossing fibers detection with an analytical high order tensor decomposition. Comput. Math. Methods Med. **2014**, 18 pp. (2014) [Article ID 476837]
21. Moakher, M.: Fourth-order Cartesian tensors: old and new facts, notions and applications. Q. J. Mech. Appl. Math. **61**(2), 181–203 (2008)

22. Ostroverkhov, V., Ostroverkhova, O., Petschek, R.G., Singer, K.D., Sukhomlinova, L., Twieg, R.J., Wang, S.-X., Chien, L.C.: Optimization of the molecular hyperpolarizability for second harmonic generation in chiral media. Chem. Phys. **257**, 263–274 (2000)
23. Özarslan, E., Mareci, T.H.: Generalized diffusion tensor imaging and analytical relationships between diffusion tensor imaging and high angular resolution diffusion imaging. Magn. Reson. Med. **50**(5), 955–965 (2003)
24. Özarslan, E., Shepherd, T.M., Vemuri, B.C., Blackband, S.J., Mareci, T.H.: Resolution of complex tissue microarchitecture using the diffusion orientation transform (DOT). NeuroImage **31**(3), 1086–1103 (2006)
25. Papenfuss, C., Ván, P.: Scalar, vectorial, and tensorial damage parameters from the mesoscopic background. Proc. Est. Acad. Sci. **57**(3), 132–141 (2008)
26. Schaeben, H.: A simple standard orientation density function: the hyperspherical de la Vallée Poussin kernel. Phys. Status Solidi (B) **200**(2), 367–376 (1997)
27. Schultz, T., Seidel, H.-P.: Estimating crossing fibers: a tensor decomposition approach. IEEE Trans. Vis. Comput. Graph. **14**(6), 1635–1642 (2008)
28. Schultz, T., Fuster, A., Ghosh, A., Deriche, R., Florack, L., Lim, L.-H.: Higher-order tensors in diffusion imaging. In: Westin, C.F., Vilanova, A., Burgeth, B. (eds.) Visualization and Processing of Tensors and Higher Order Descriptors for Multi-Valued Data. Mathematics and Visualization, pp. 129–161. Springer, Berlin/Heidelberg (2014)
29. Snieder, R.: A Guided Tour of Mathematical Methods for the Physical Sciences, 2nd edn. Cambridge University Press, Cambridge (2001)
30. Tournier, J.-D., Calamante, F., Gadian, D.G., Connelly, A.: Direct estimation of the fiber orientation density function from diffusion-weighted MRI data using spherical deconvolution. NeuroImage **23**(3), 1176–1185 (2004)
31. Tuch, D.S.: Q-ball imaging. Magn. Reson. Med. **52**(6), 1358–1372 (2004)
32. van der Boogaart, K.G., Hielscher, R., Prestin, J., Schaeben, H.: Kernel-based methods for inversion of the Radon transform on SO(3) and their applications to texture analysis. J. Comput. Appl. Math. **199**, 122–140 (2007)
33. Voyiadjis, G.Z., Kattan, P.I.: Evolution of fabric tensors in damage mechanics of solids with micro-cracks: Part I - Theory and fundamental concepts. Mech. Res. Commun. **34**(2), 145–154 (2007)
34. Wang, B., Zhou, J., Koschny, T., Kafesaki, M., Soukoulis, C.M.: Chiral metamaterials: simulations and experiments. J. Opt. A Pure Appl. Opt. **11**, 114003 (2009)
35. Watson, G.S.: Distributions on the circle and sphere. J. Appl. Probab. **19**, 265–280 (1982)